Multi-hadron states from elongated boxes

Andrei Alexandru
Michael Döring, Maxim Mai, Chris Culver

Multihadron dynamics in a box
Bethe Center for Theoretical Physics
Bonn, September 2019

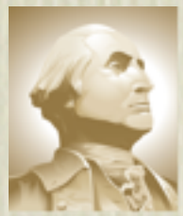

THE GEORGE WASHINGTON UNIVERSITY
WASHINGTON, DC

Outline

- Motivation
- Two-body scattering from lattice QCD
- Results for 2π spectrum and phase shifts for I=0,1,2
- Resonance parameters from fits
- Conclusions and future directions

Motivation

- 'Resonances' are unstable hadronic excitations that play an important role in hadron interactions.
- Currently the resonances are determined from PWA of experimental data coupled with modeling.
- Resonances appear as sharp features in phase-shift or cross-section data.
- The spectrum of hadronic resonances is an open problem: expected baryonic resonances are missing, exotic resonances are expected in light and charmed mesons, etc.

Scattering from lattice QCD

Final state interactions from euclidean correlation functions ☆

L. Maiani
Dipartimento di Fisica, Università di Roma "La Sapienza", and Istituto Nazionale di Fisica Nucleare, Sezione di Roma, I-00185 Rome, Italy

and

M. Testa
Dipartimento di Fisica, Università di Lecce, and Istituto Nazionale di Fisica Nucleare, Sezione di Lecce, I-73100 Lecce, Italy

$$F_q^{\mathrm{conn}}(t_2) = \frac{\sqrt{Z_\pi}}{\sqrt{2E_q}} \exp(-E_q t_2)$$

$$\times \left(\tfrac{1}{2} \sum_n (2\pi)^4 \delta^3(\boldsymbol{P}_n) \delta(E_n - 2E_q) [\mathrm{i}\mathcal{M}(\boldsymbol{q}, -\boldsymbol{q}; n)]^* \langle n, \mathrm{out}|J(0)|0\rangle + P_q(t_2) \right), \tag{19}$$

$$P_q(t_2) = -\wp \sum_n \exp[-(E_n - 2E_q)t_2](2\pi)^3 \delta^3(\boldsymbol{P}_n) N_n \frac{[\mathcal{M}(\boldsymbol{q}, -\boldsymbol{q}; n)]^* \langle n; \mathrm{out}|J(0)|0\rangle}{E_n(E_n - 2E_q)}, \tag{20}$$

$$\boldsymbol{P}_q(t_2) \underset{t_2 \to +\infty}{\sim} \exp[2(E_q - M_\pi)t_2] \tag{22}$$

Scattering from lattice QCD

- In a finite box the energy of two-hadron states is modified by their interaction.
- Lattice QCD can be used to determine the energy of these states in finite boxes.
- Lüscher formula connects this finite volume effect to scattering phase-shifts.
- The symmetry group of the box dictates the spectral decomposition and plays a key role in the connection to phase-shifts.

Lüscher formula

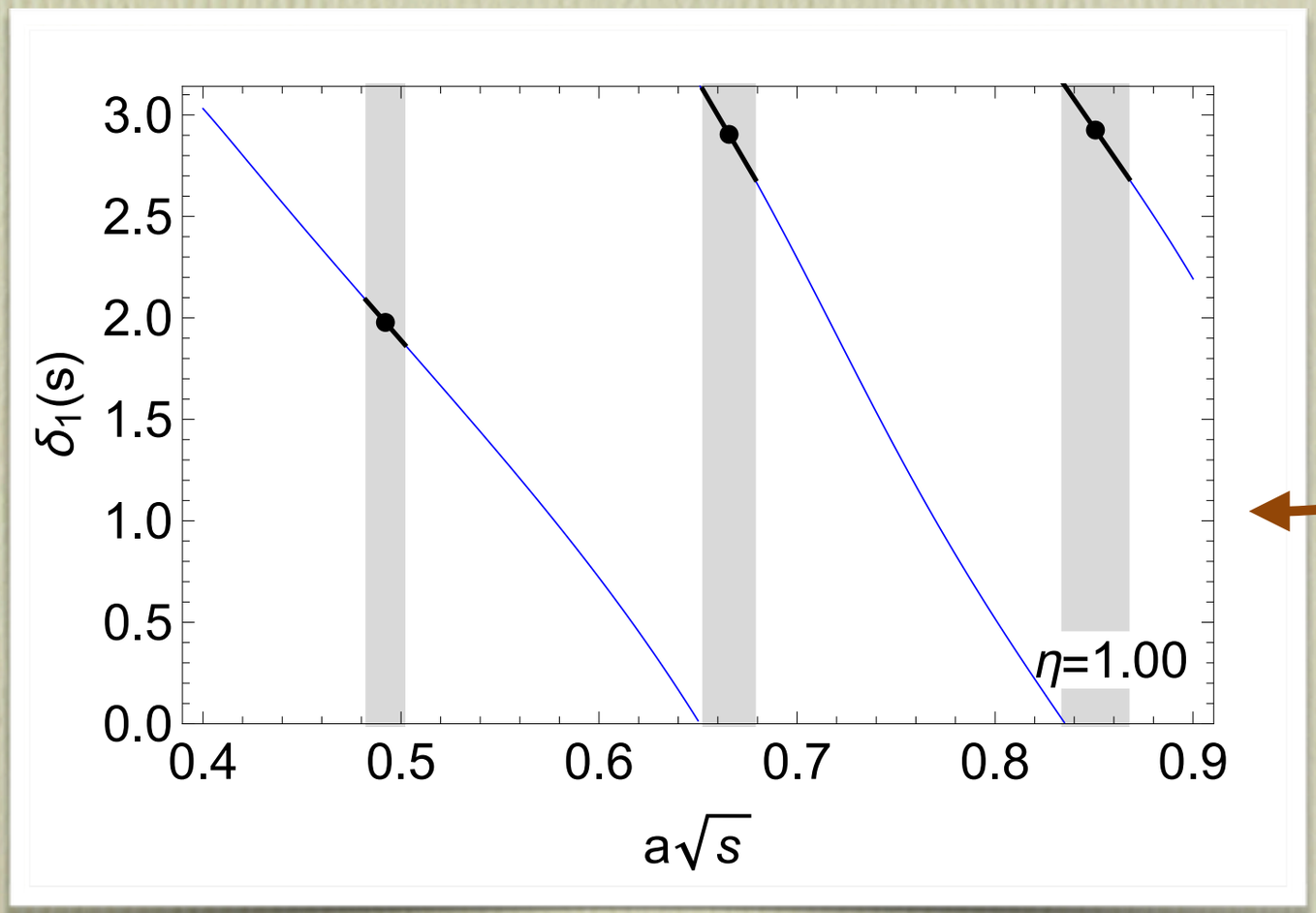

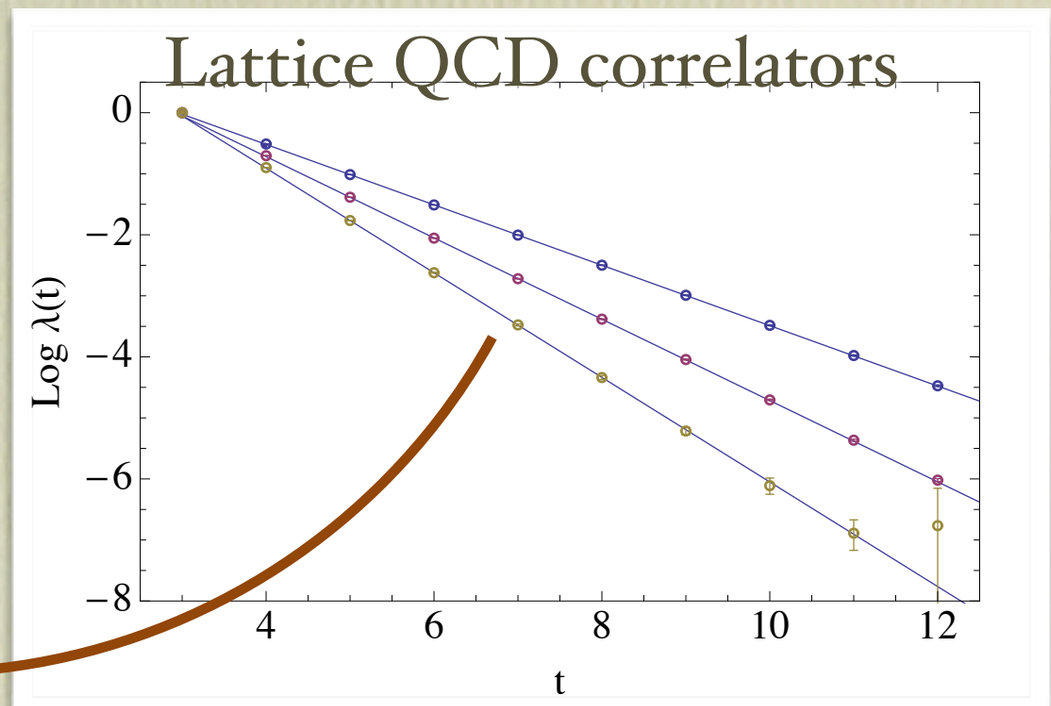

$$\mathbf{A_2^-}: \qquad \cot\delta_1(k) = \mathcal{W}_{00} + \frac{2}{\sqrt{5}}\mathcal{W}_{20}\ ,$$

$$\mathcal{W}_{lm}(1,q^2;\eta) = \frac{\mathcal{Z}_{lm}(1,q^2;\eta)}{\pi^{3/2}\eta q^{l+1}}\ .$$

X. Feng, X. Li, and C. Liu, Phys.Rev. D70 (2004) 014505

Lüscher formula

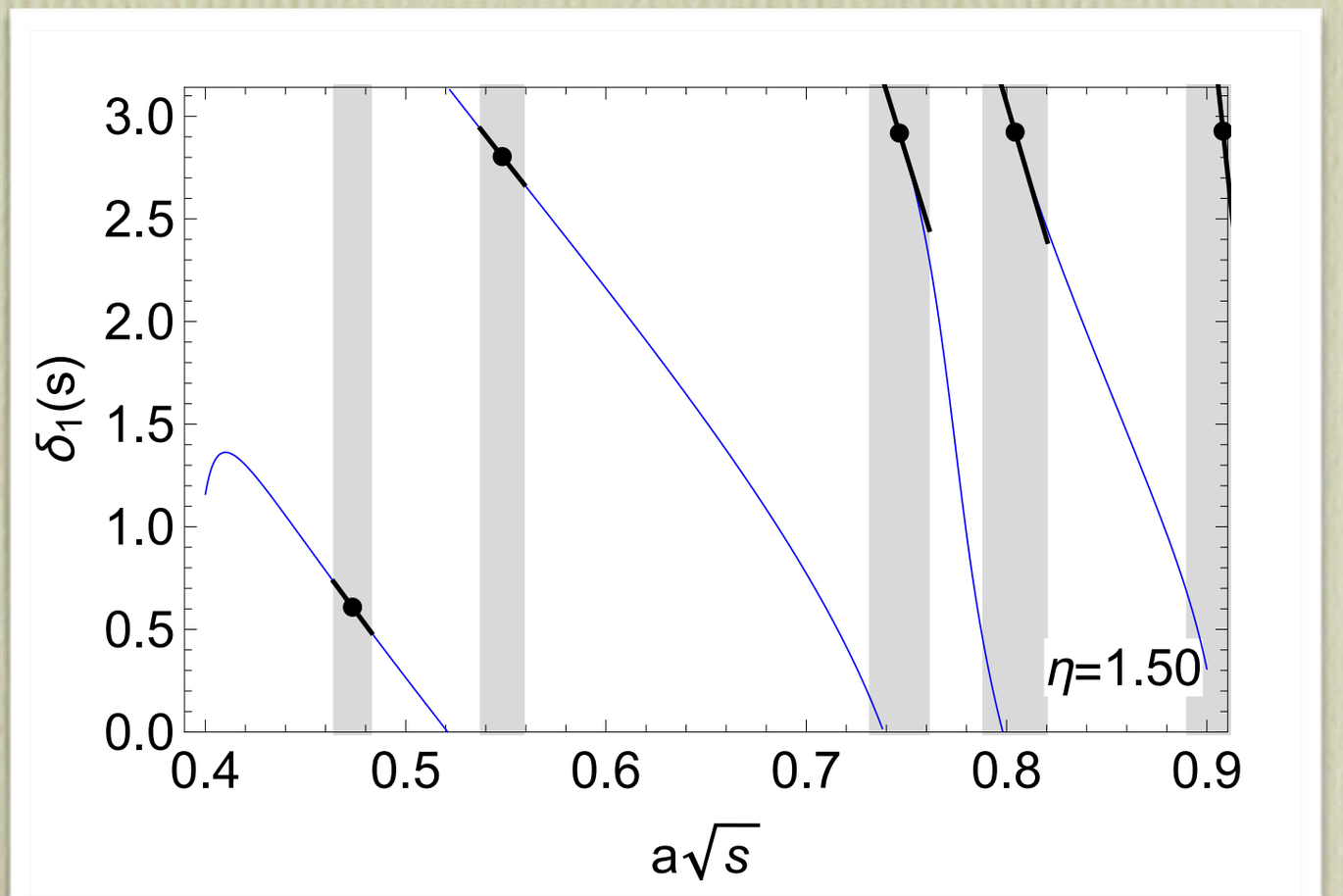

$$\mathbf{A_2^-}: \qquad \cot\delta_1(k) = \mathcal{W}_{00} + \frac{2}{\sqrt{5}}\mathcal{W}_{20}\ ,$$

$$\mathcal{W}_{lm}(1,q^2;\eta) = \frac{\mathcal{Z}_{lm}(1,q^2;\eta)}{\pi^{3/2}\eta q^{l+1}}\ .$$

Lüscher formula

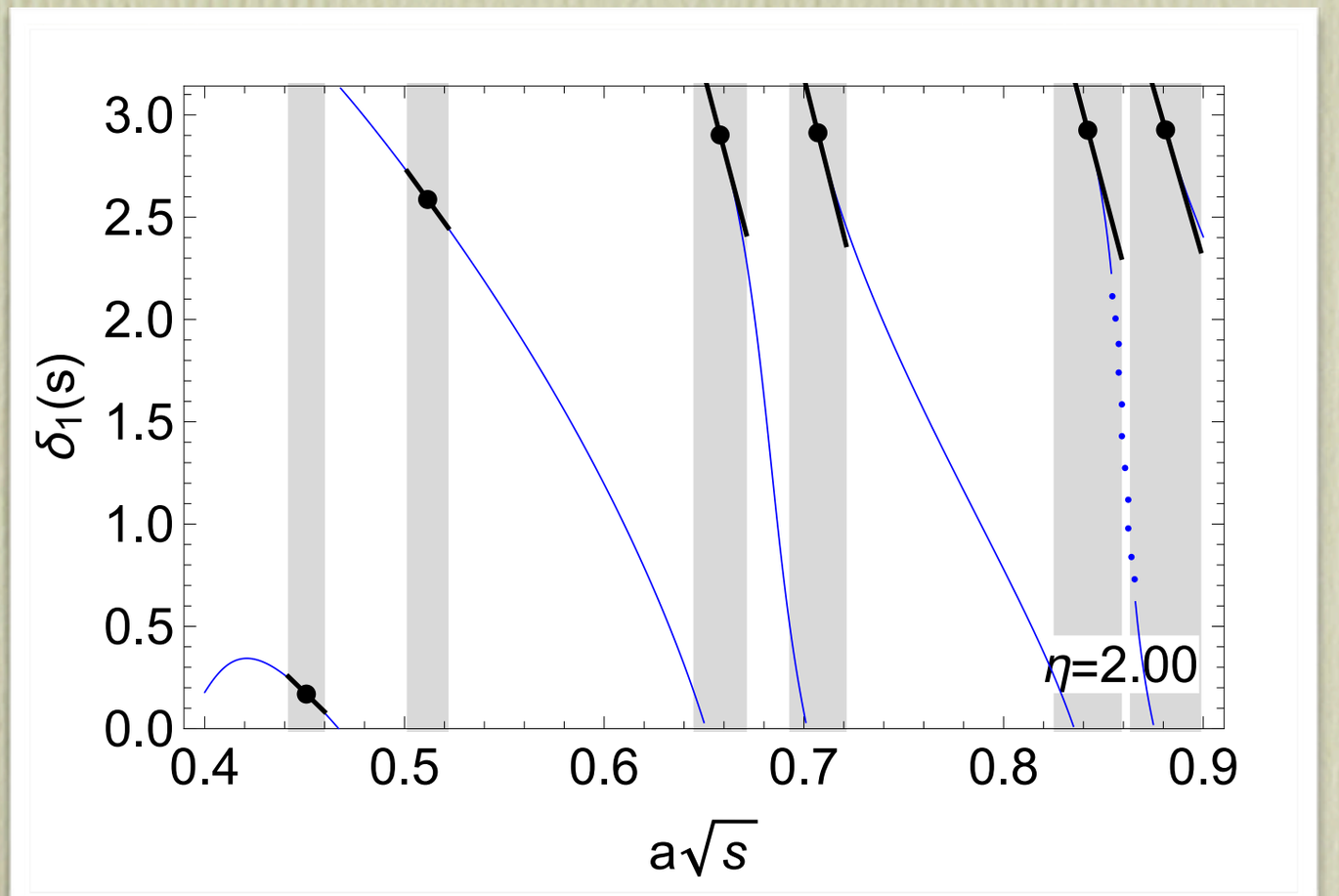

$$\mathbf{A_2^-}: \qquad \cot\delta_1(k) = \mathcal{W}_{00} + \frac{2}{\sqrt{5}}\mathcal{W}_{20}\ ,$$

$$\mathcal{W}_{lm}(1,q^2;\eta) = \frac{\mathcal{Z}_{lm}(1,q^2;\eta)}{\pi^{3/2}\eta q^{l+1}}\ .$$

Phase shifts

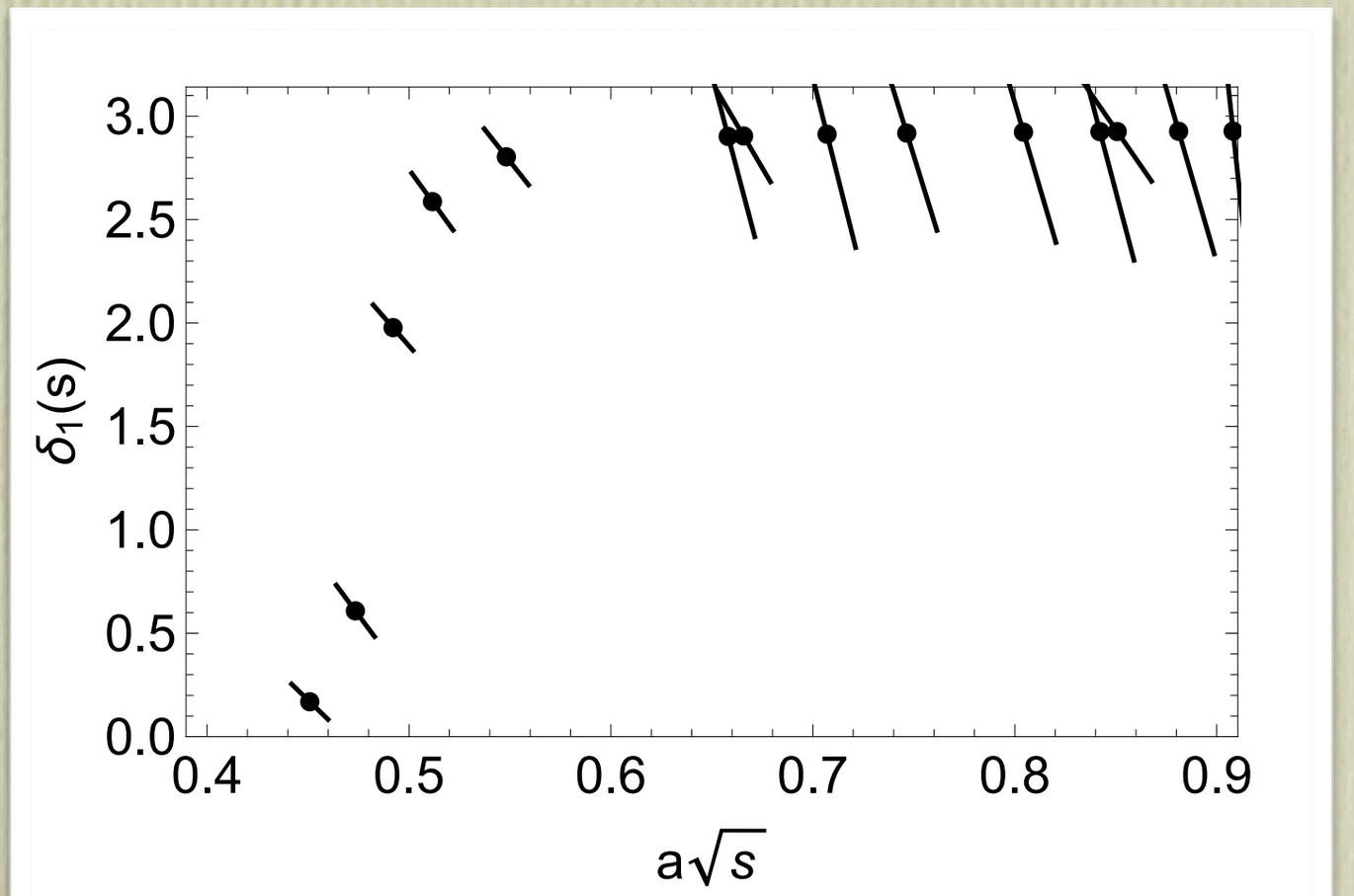

Resonance parameters

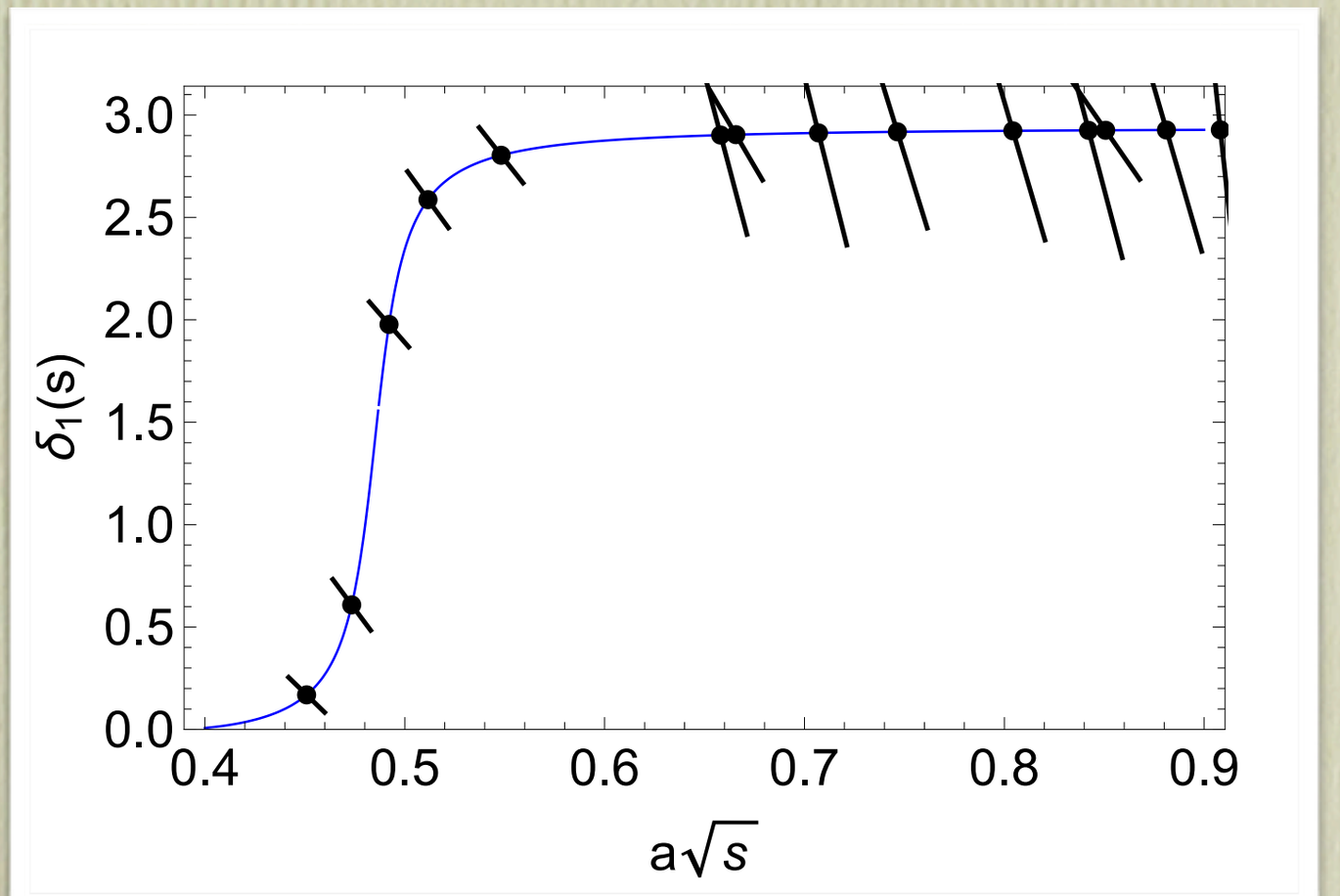

Breit-Wigner parametrization

$$\tan\delta = \frac{E_{cm}\Gamma(E_{cm})}{m_\rho^2 - E_{cm}^2}$$

$$\Gamma(E_{cm}) = \frac{g_{\rho\pi\pi}^2}{6\pi}\frac{p_{cm}^3}{E_{cm}^2}$$

Resonance parameters energy space

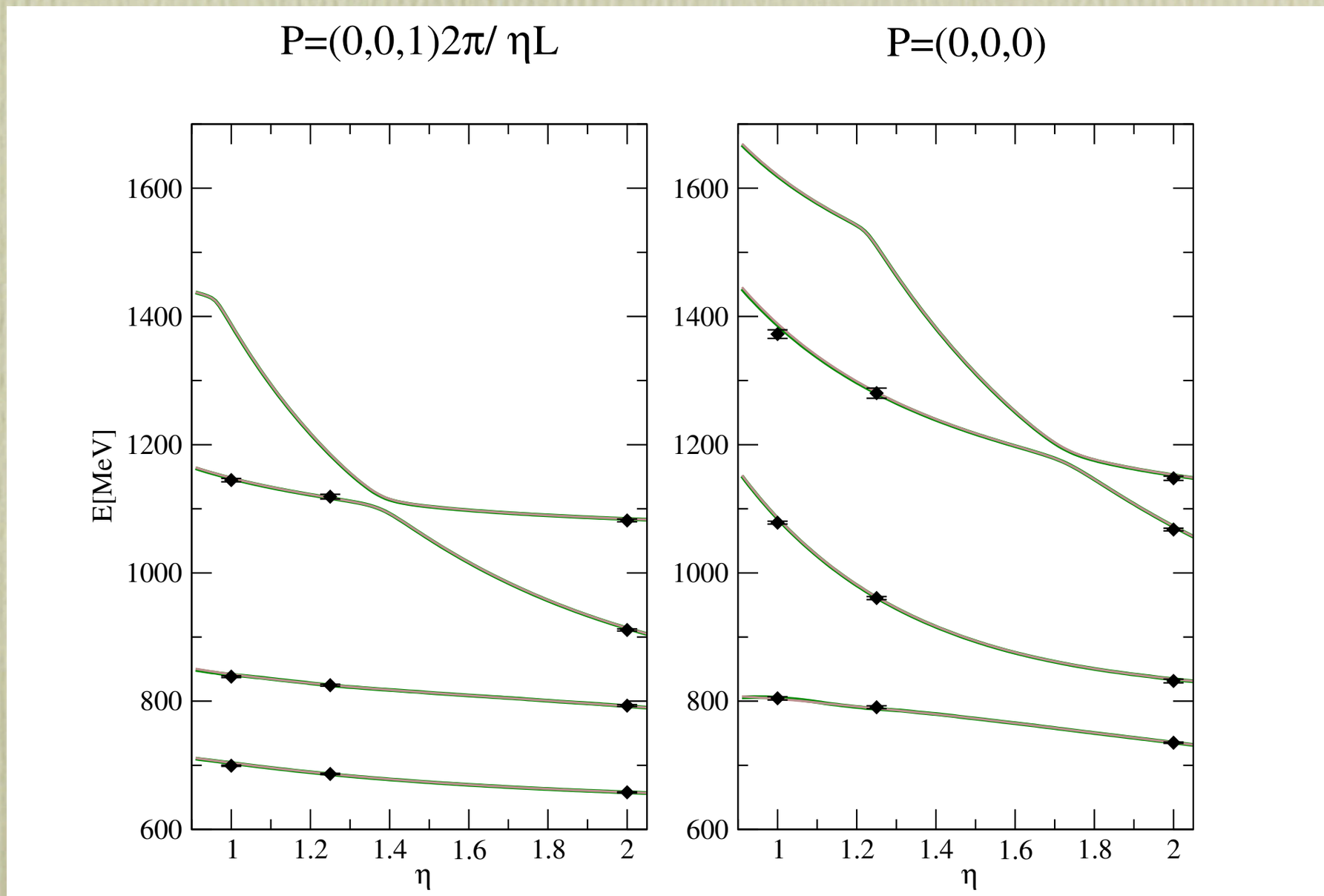

Simulations parameters

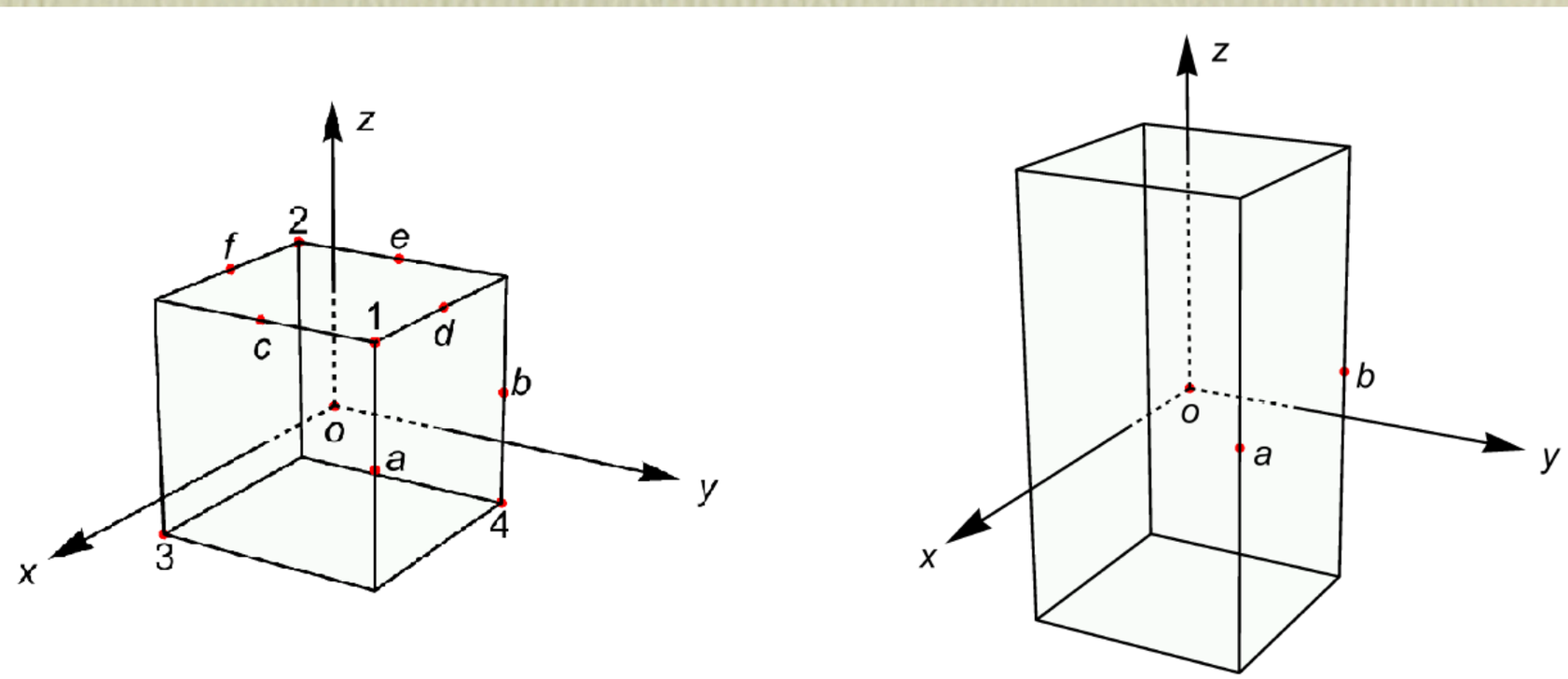

ensemble	$N_t \times N_{x,y}^2 \times N_z$	η	a[fm]	$N_{\rm cfg}$	aM_π	am_N	$am_{u/d}^{pcac}$	af_π
$\mathcal{E}_1$	$48 \times 24^2 \times 24$	1.0	0.1210(2)(24)	300	0.1934(5)	0.644(6)	0.01237(9)	0.0648(8)
$\mathcal{E}_2$	$48 \times 24^2 \times 30$	1.25	–	–	–	–	–	–
$\mathcal{E}_3$	$48 \times 24^2 \times 48$	2.0	–	–	–	–	–	–
$\mathcal{E}_4$	$64 \times 24^2 \times 24$	1.0	0.1215(3)(24)	400	0.1390(5)	0.62(1)	0.00617(9)	0.060(1)
$\mathcal{E}_5$	$64 \times 24^2 \times 28$	1.17	–	–	–	–	–	–
$\mathcal{E}_6$	$64 \times 24^2 \times 32$	1.33	–	–	–	–	–	–

Symmetry considerations

- The symmetry group for zero-momentum states in elongated boxes is D_{4h}
- There are 16 elements in the group
- 8 1-dim irreps: $\mathbf{A_1^{\pm}}$, $\mathbf{A_2^{\pm}}$, $\mathbf{B_1^{\pm}}$, $\mathbf{B_2^{\pm}}$ and 2 2-dim irreps $\mathbf{E^{\pm}}$
- For J=1 the relevant irreps are a 2-dim $\mathbf{E^-}$ and 1-dim $\mathbf{A_2^-}$
- For J=0 the relevant irrep is $\mathbf{A_1^+}$

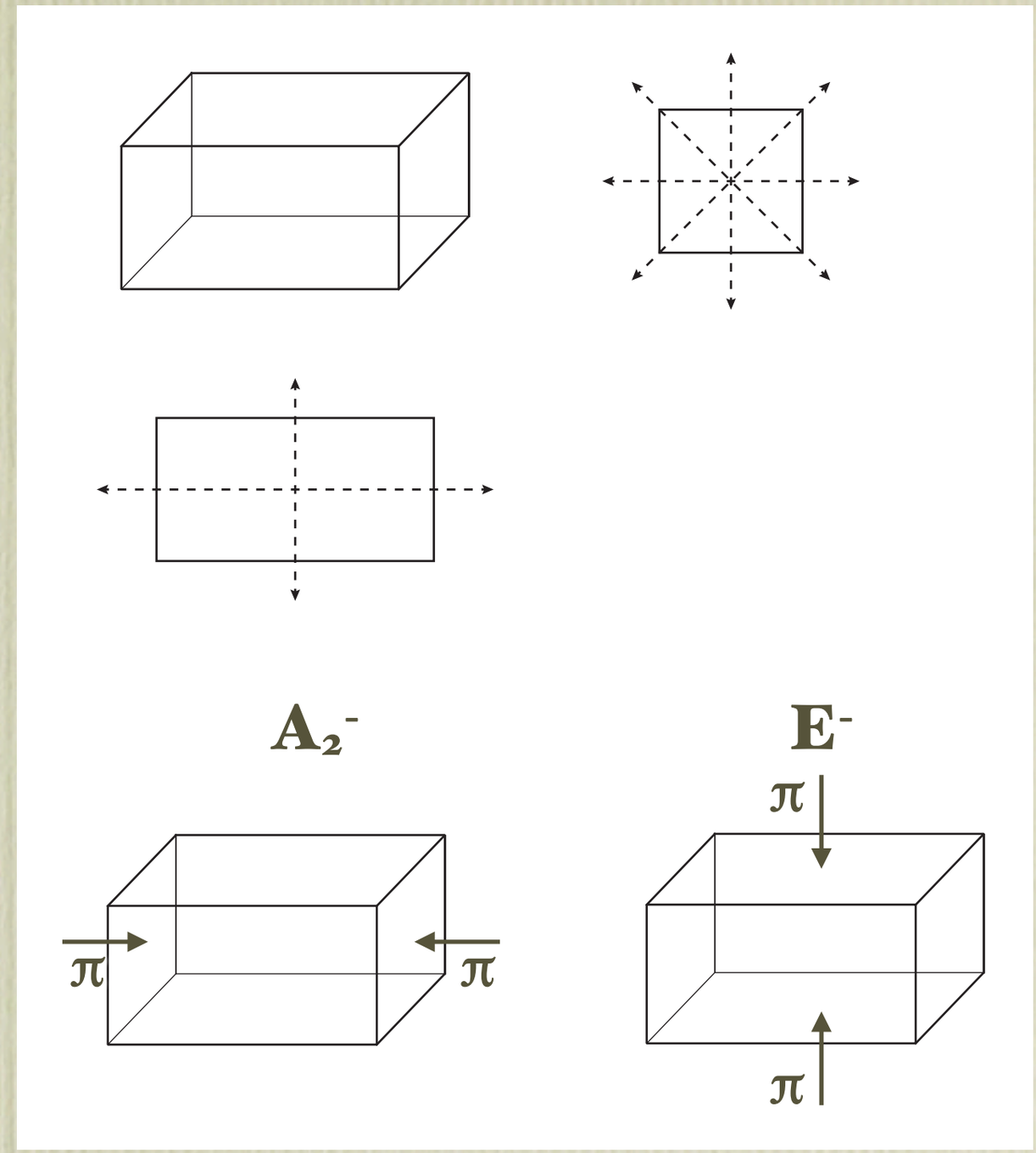

Symmetry considerations

TABLE I. Resolution of the $2J + 1$ spherical harmonics into the irreducible representations of O_h and D_{4h}.

J	O_h	D_{4h}
0	A_1^+	A_1^+
1	F_1^-	$A_2^- \oplus E^-$
2	$E^+ \oplus F_2^+$	$A_1^+ \oplus B_1^+ \oplus B_2^+ \oplus E^+$
3	$A_2^- \oplus F_1^- \oplus F_2^-$	$A_2^- \oplus B_1^- \oplus B_2^- \oplus 2E^-$
4	$A_1^+ \oplus E^+ \oplus F_1^+ \oplus F_2^+$	$2A_1^+ \oplus A_2^+ \oplus B_1^+ \oplus B_2^+ \oplus 2E^+$

For J=0 the relevant irrep is the 1-dim $\mathbf{A_1^+}$ for both cubic and elongated boxes.

On the lattice this irrep mixes also with J=4 and J=2 for cubic and elongated boxes respectively.

Variational method

- When the energy states are nearly degenerate, as is the case in scattering spectra, exponential fitting is an ill posed problem.

$$\langle 0|O(t)O(0)|0\rangle = |\langle 1|O|0\rangle|^2 e^{-E_1 t} + |\langle 2|O|0\rangle|^2 e^{-E_2 t} + \cdots$$

- The workaround is to use information from a set of interpolating fields.

$$\begin{aligned}
\langle 0|O_1(t)O_1(0)|0\rangle &= c_{11}c_{11}^* e^{-E_1 t} + c_{12}c_{12}^* e^{-E_2 t} + \cdots \\
\langle 0|O_2(t)O_2(0)|0\rangle &= c_{21}c_{21}^* e^{-E_1 t} + c_{22}c_{22}^* e^{-E_2 t} + \cdots \\
\langle 0|O_1(t)O_2(0)|0\rangle &= c_{11}c_{21}^* e^{-E_1 t} + c_{12}c_{22}^* e^{-E_2 t} + \cdots
\end{aligned}$$

- The problem is then solved using a generalized eigenvalue problem.

$$C(t)v(t) = \lambda(t)C(0)v(t) \quad \text{with} \quad C(t) = \begin{pmatrix} \langle 0|O_1(t)O_1(0)|0\rangle & \langle 0|O_1(t)O_2(0)|0\rangle \\ \langle 0|O_2(t)O_1(0)|0\rangle & \langle 0|O_2(t)O_2(0)|0\rangle \end{pmatrix}$$

Operator basis for I=1

$$\rho_i^{\mathrm{I}}(t) = \frac{1}{\sqrt{2}}\left[\bar{u}(t)\gamma_i e^{i\mathbf{p}}u(t) - u \leftrightarrow d\right]$$

$$\rho_i^{\mathrm{II}}(t) = \frac{1}{\sqrt{2}}\left[\bar{u}(t)\gamma_4\gamma_i e^{i\mathbf{p}}u(t) - u \leftrightarrow d\right]$$

$$\rho_i^{\mathrm{III}}(t) = \frac{1}{\sqrt{2}}\left[\bar{u}(t)\nabla_j\gamma_i e^{i\mathbf{p}}\nabla_j u(t) - u \leftrightarrow d\right]$$

$$\rho_i^{\mathrm{IV}}(t) = \frac{1}{\sqrt{2}}\left[\bar{u}(t)\frac{1}{2}\{e^{i\mathbf{p}},\nabla_i\}u(t) - u \leftrightarrow d\right]$$

$$\pi\pi(p_1,p_2,t) = \frac{1}{\sqrt{2}}[\pi^+(p_1)\pi^-(p_2) - \pi^+(p_2)\pi^-(p_1)]$$

- These are operators with I=1 and I_3=0.
- Linear combinations that change under A_2^- are used (e.g. γ_1 for ϱ and $p_1=-p_2=[1,0,0]$ for $\pi\pi$).

Correlation functions

$$\left\langle \Omega \left| \rho_i(t) \rho_j^\dagger(0) \right| \Omega \right\rangle = -$$

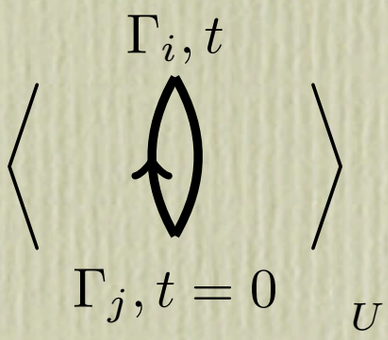

$$_U$$

$$\left\langle \Omega \left| \rho_i(p_1 + p_2, t), \pi\pi(p_1, p_2, 0)^\dagger \right| \Omega \right\rangle =$$

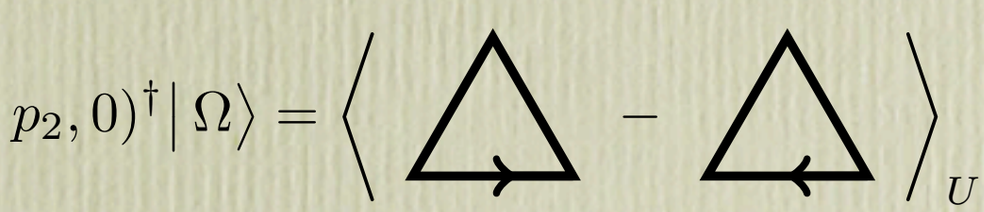

$$_U$$

$$\left\langle \Omega \left| \pi\pi(p_1, p_2, t) \pi\pi(p_1, p_2, 0)^\dagger \right| \Omega \right\rangle =$$

$$-$$

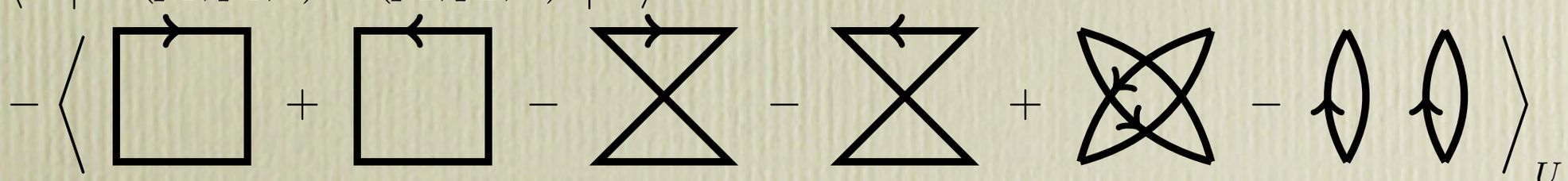

$$_U$$

LapH details

$$\Delta\,|\lambda\rangle = \lambda\,|\lambda\rangle\ , \qquad -12 \le \lambda \le 0$$

$$S(\Lambda) = \sum_{-\lambda<\Lambda} |\lambda\rangle\,\langle\lambda|$$

$$|\psi\rangle_s = S(\Lambda)\,|\psi\rangle = \sum_{-\lambda<\Lambda} \langle\lambda|\psi\rangle\,|\lambda\rangle$$

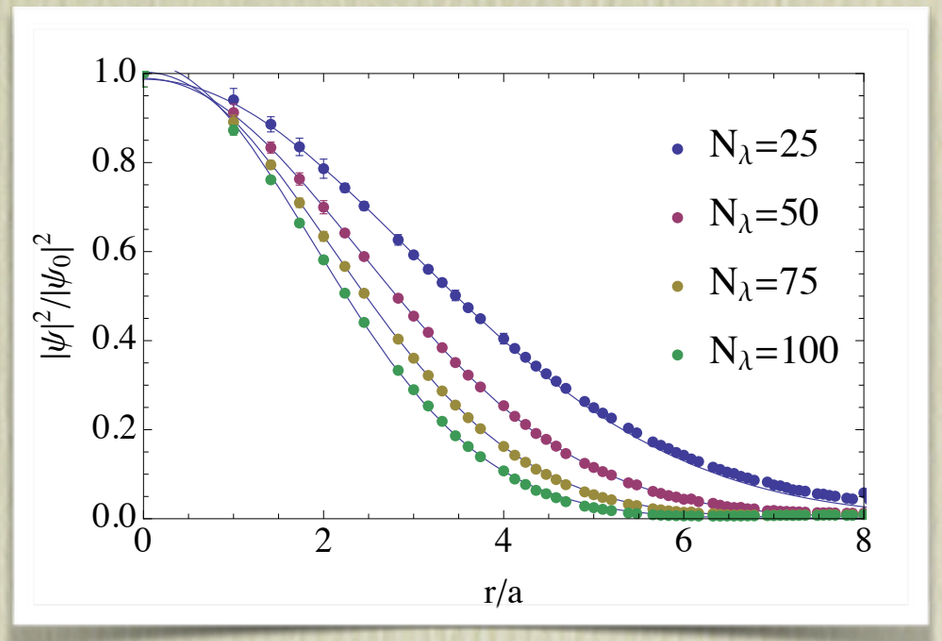

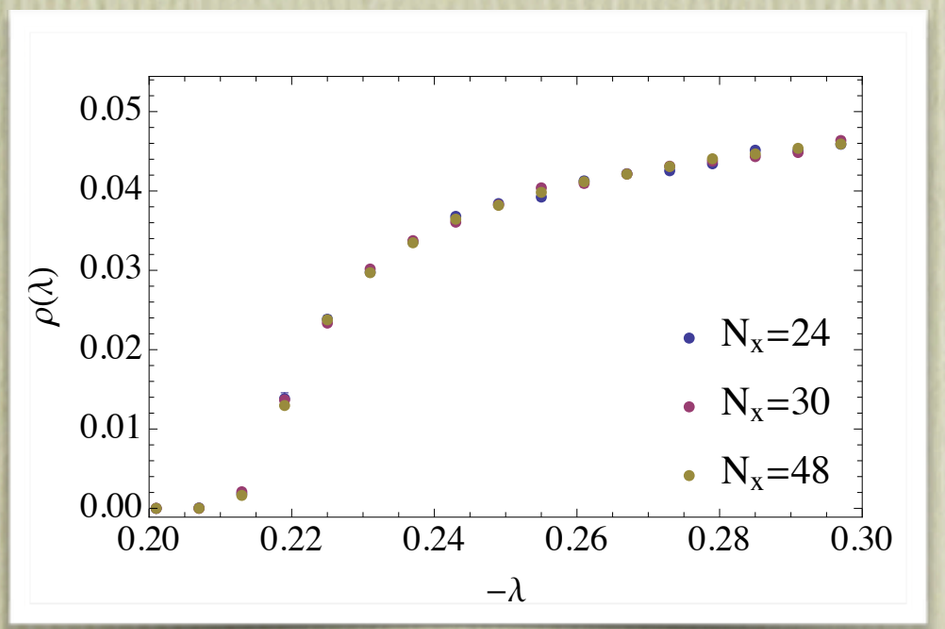

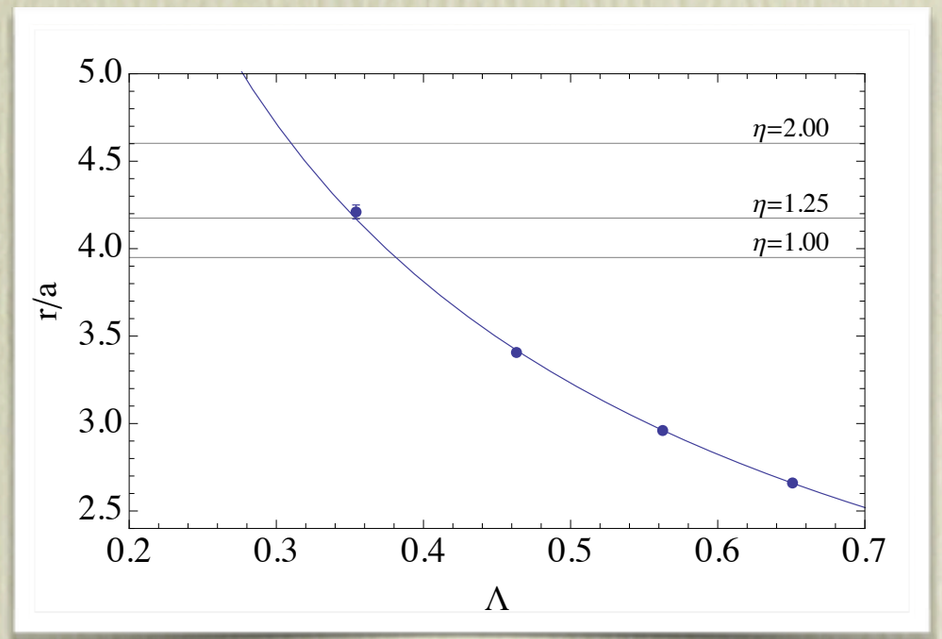

M. Peardon et. al., Phys.Rev. D80 (2009) 054506

Energy level extraction

$$C_{ij}(t) = \left\langle \Omega \left| O_i(t) O_j(0)^\dagger \right| \Omega \right\rangle$$
$$\tilde{C}(t, t_0) = C(t_0)^{-1/2} C(t) C(t_0)^{-1/2}$$
$$\tilde{C}(t, t_0)\psi_i(t) = \lambda_i(t)\psi_i(t)$$
$$\lambda_i(t) \propto e^{-E_i t}$$

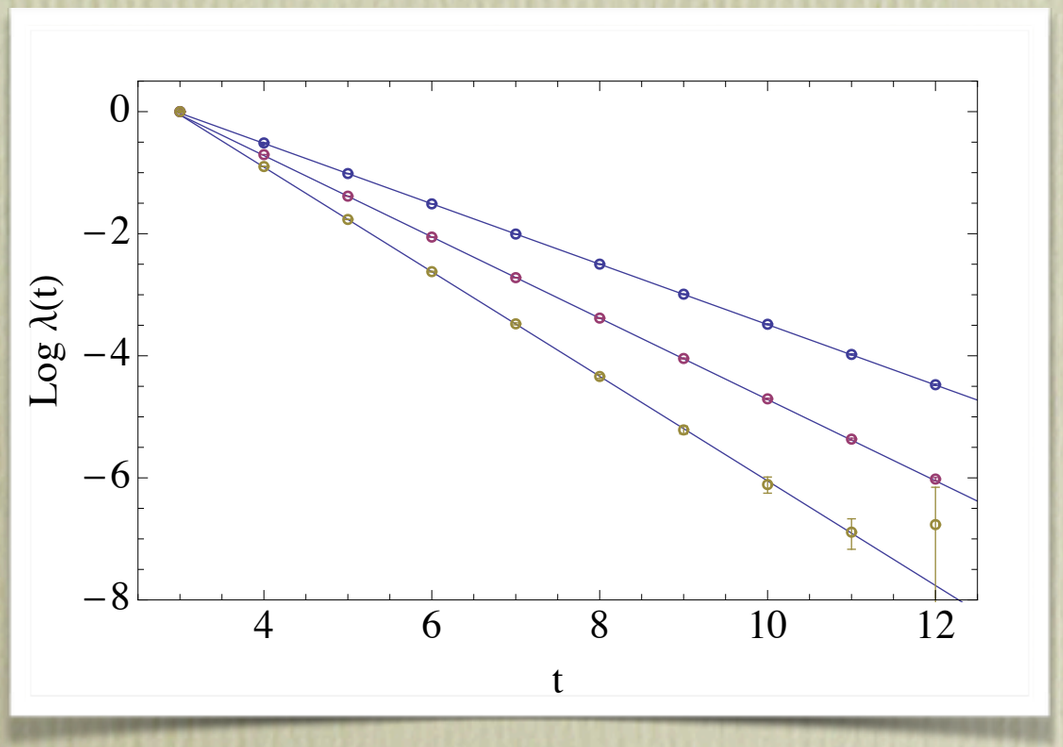

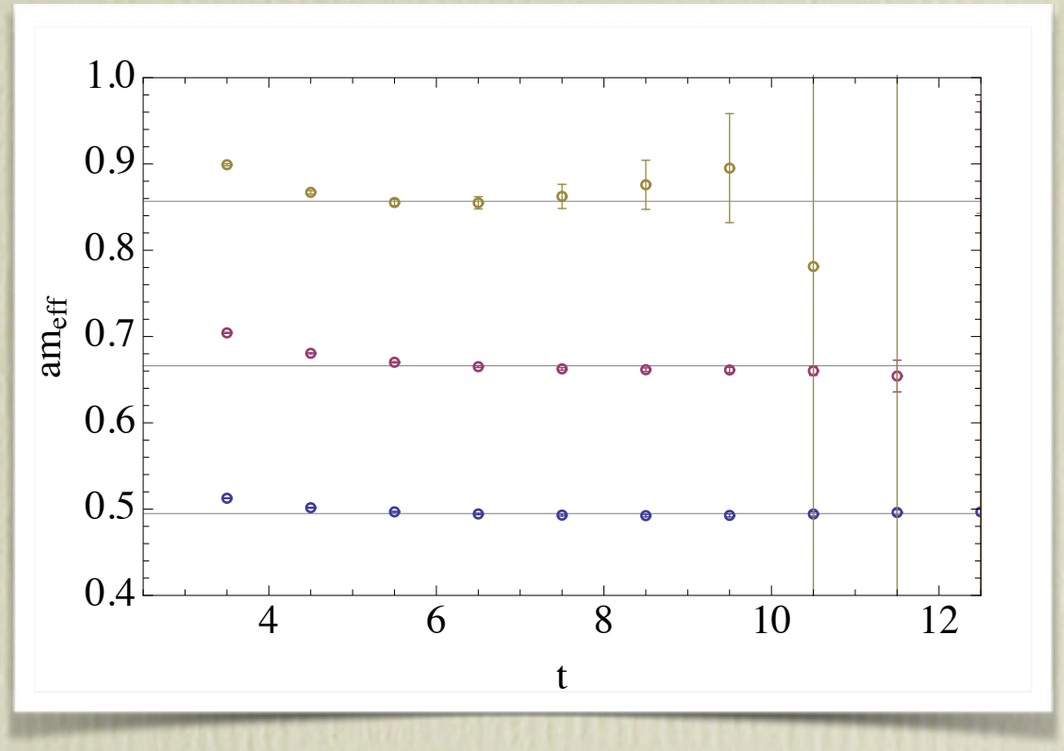

Energy level extraction - thermal effects

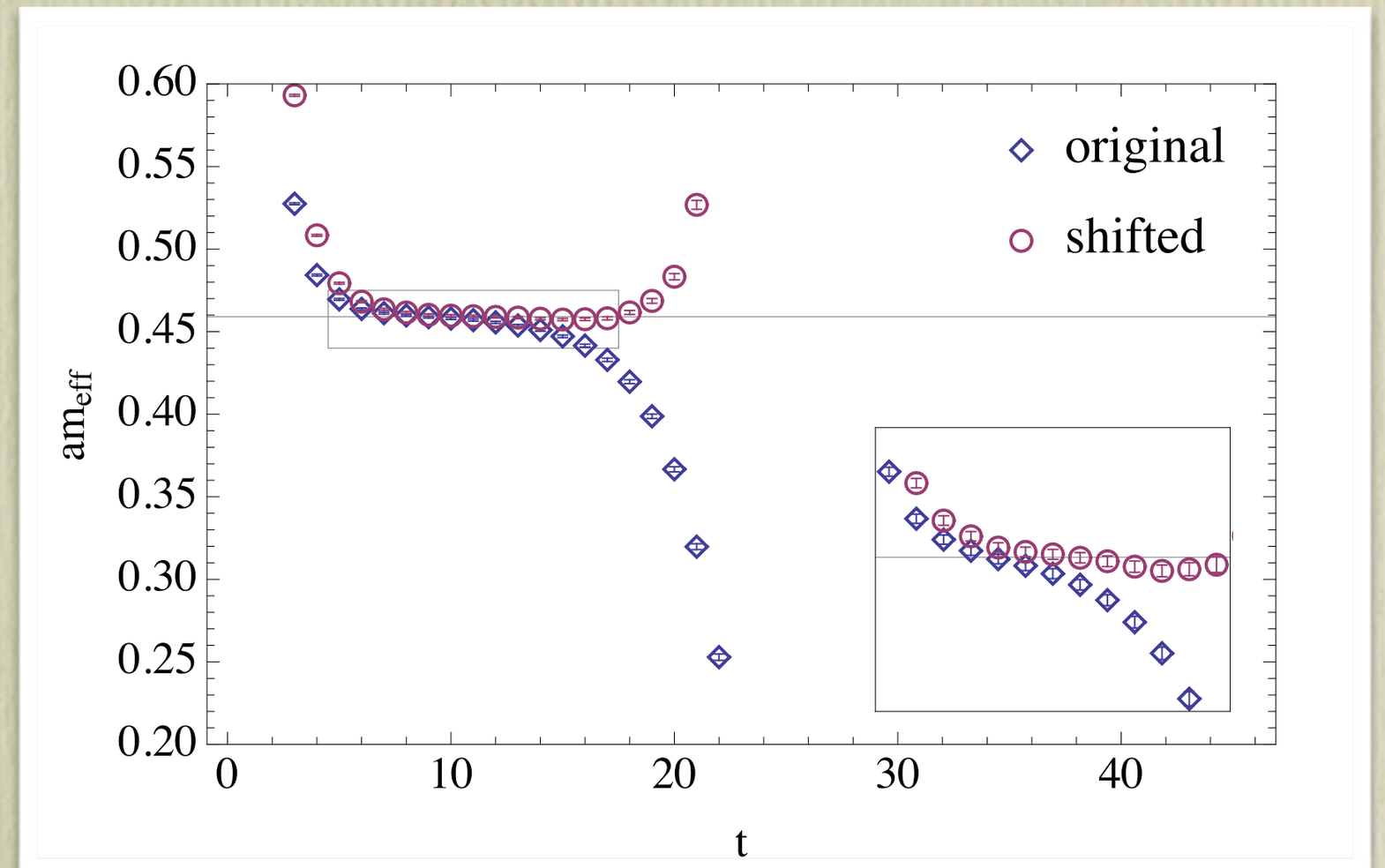

$$G_s(t) = G(t) - G(t + \delta t)$$

$$m_{\text{eff}} = -\log \frac{G_s(t+1)}{G_s(t)}$$

Interpolating fields - stability

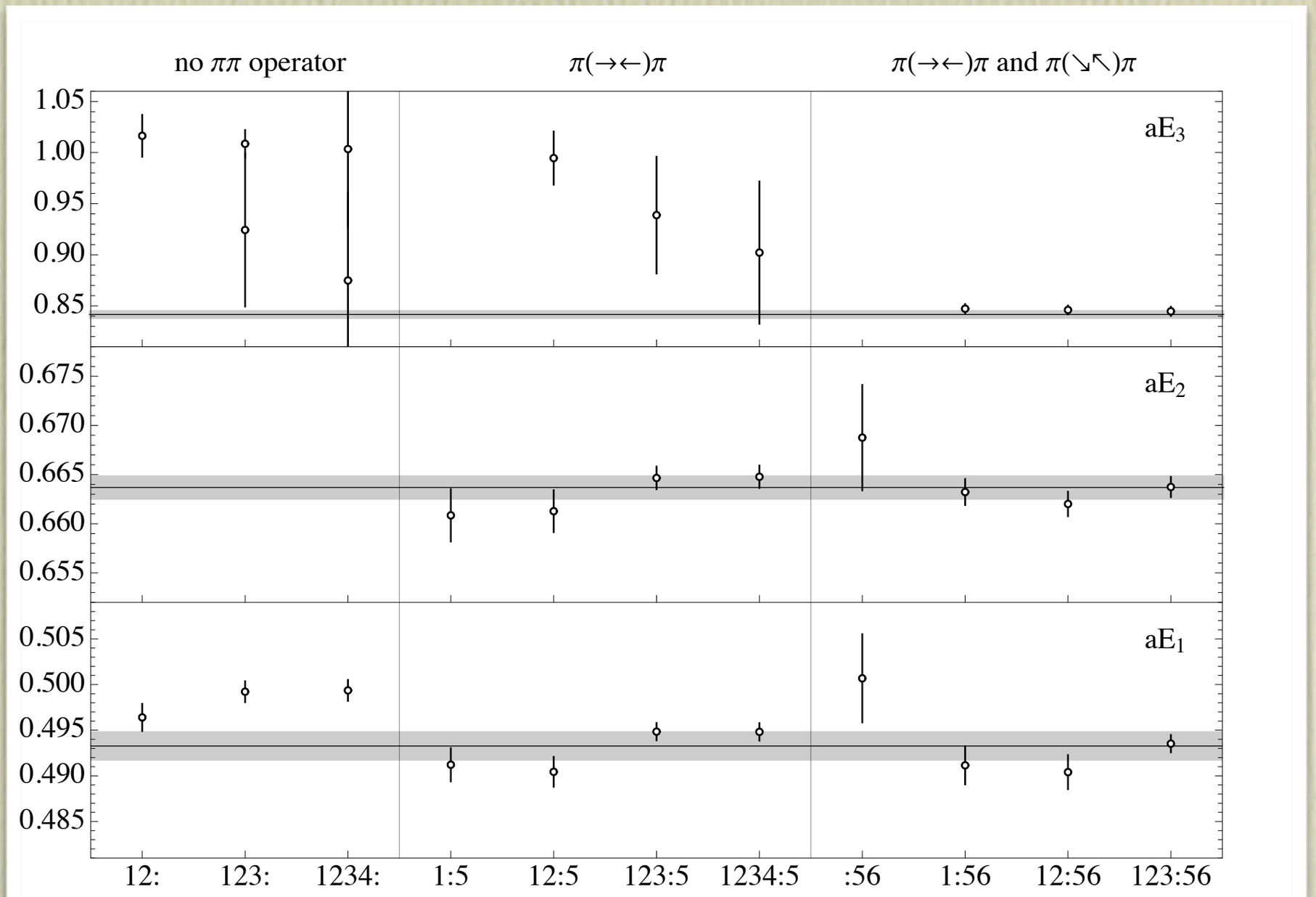

I=1 phase shifts (ϱ region)

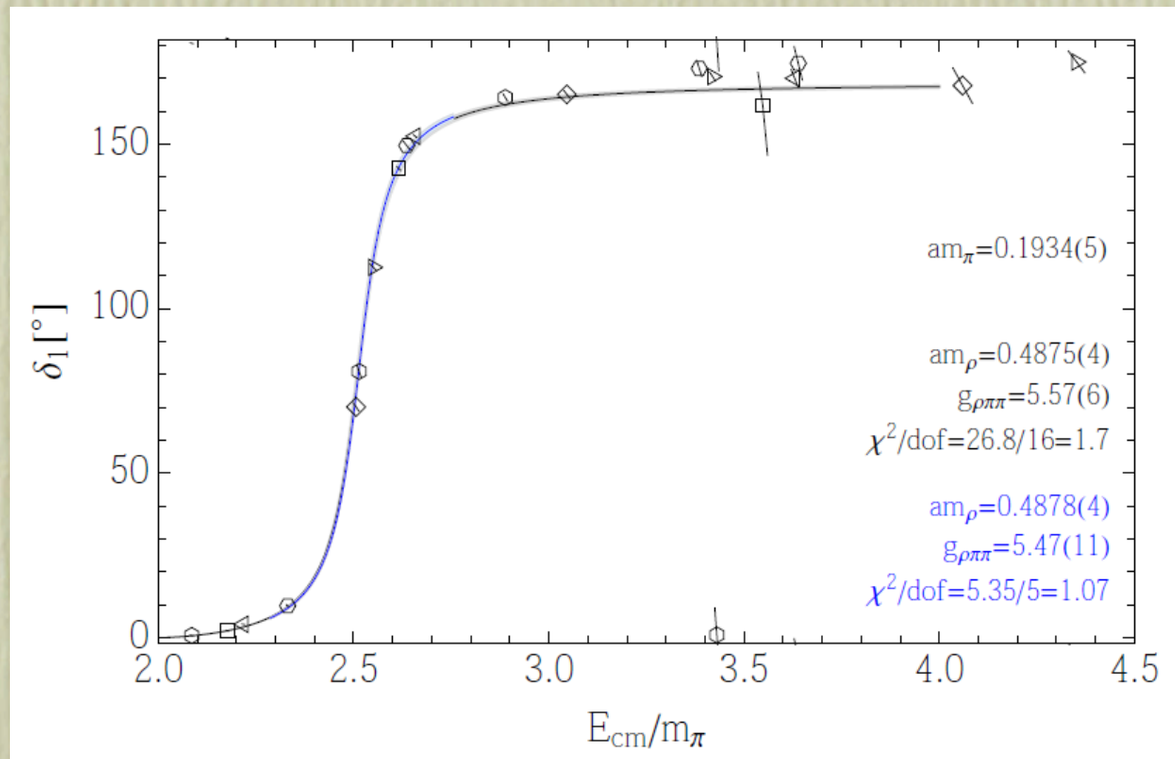

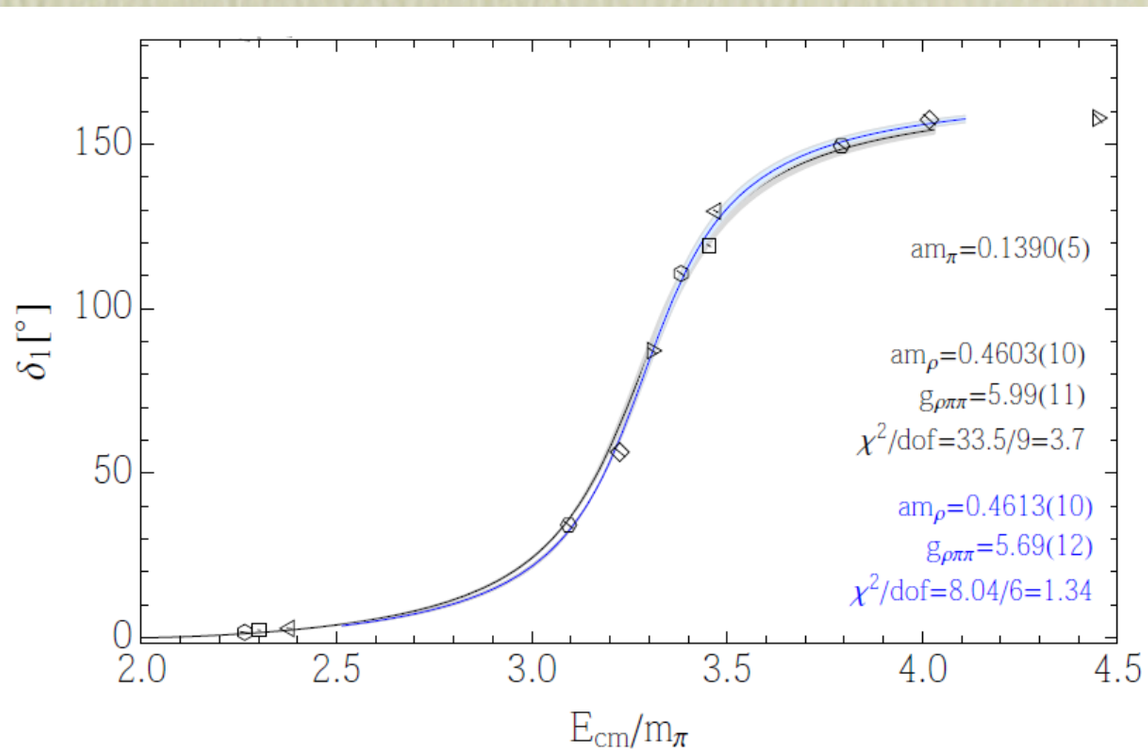

C. Pelissier and AA, Phys.Rev. D87 (2013) 014503, [arXiv:1211.0092].

D. Guo, AA, R. Molina, and M. Doering, Phys. Rev. D94 (2016), no. 3 034501, [arXiv:1605.03993].

Phase shift - model fits

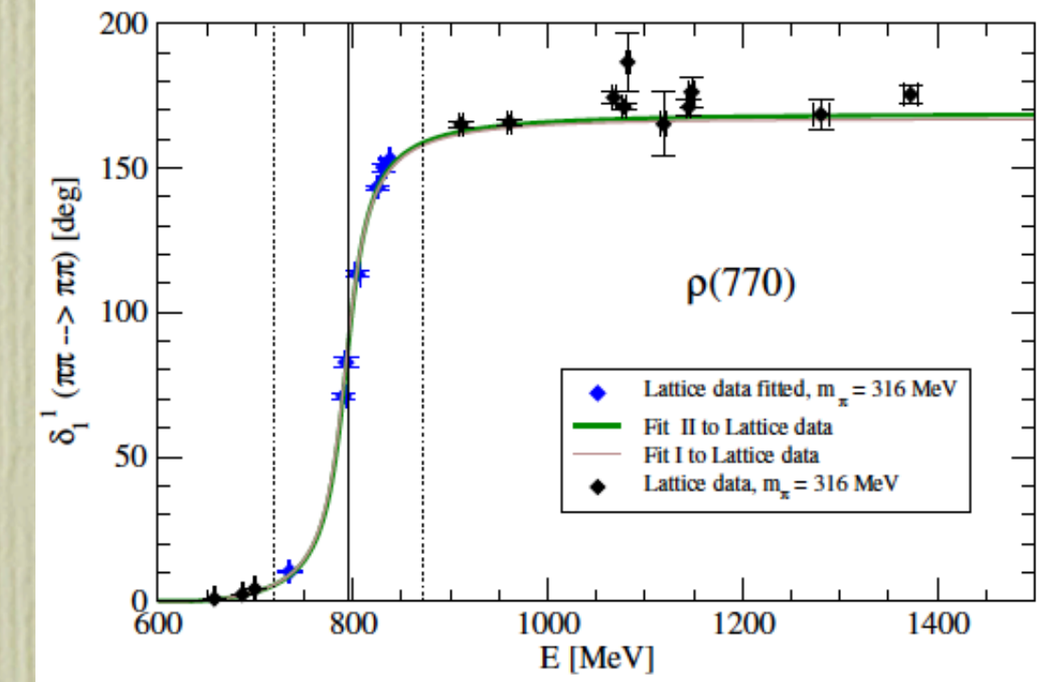

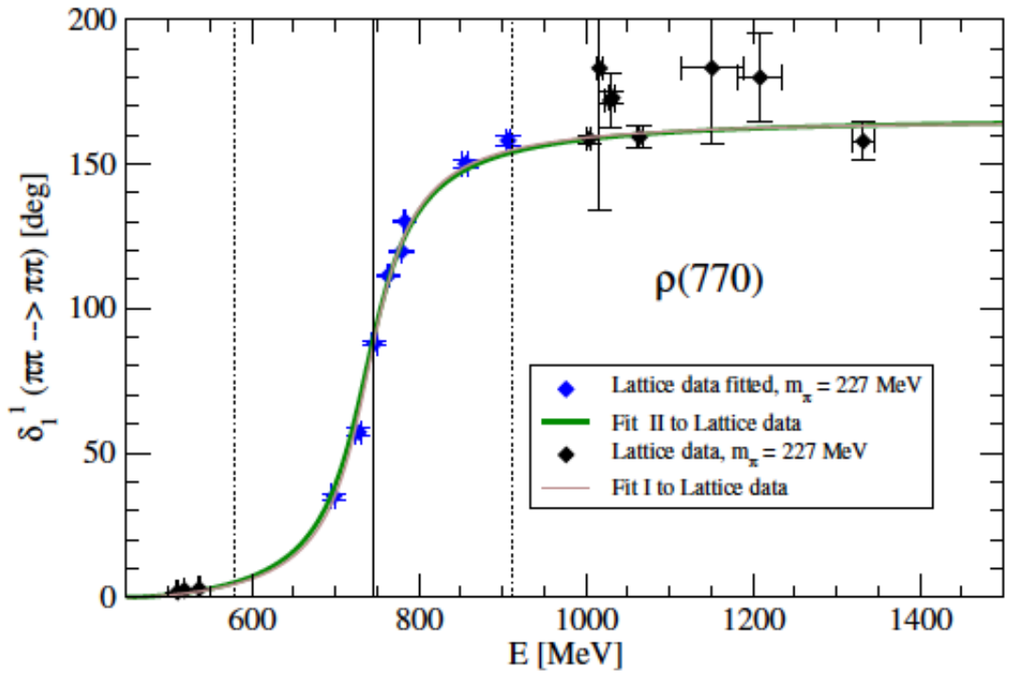

	m_π	m_ρ	Γ_ρ	g	χ^2/dof
Breit Wigner	315	794.661	36.98	5.57	2.16
K-matrix		795.746	35.90	5.465	0.82
UχPT		794.481	36.06		1.26
Breit Wigner	227	748.354	70.27	5.7	1.46
K-matrix		748.216	80.25	5.683	1.28
UχPT		746.451	76.95		1.53

Chiral extrapolation

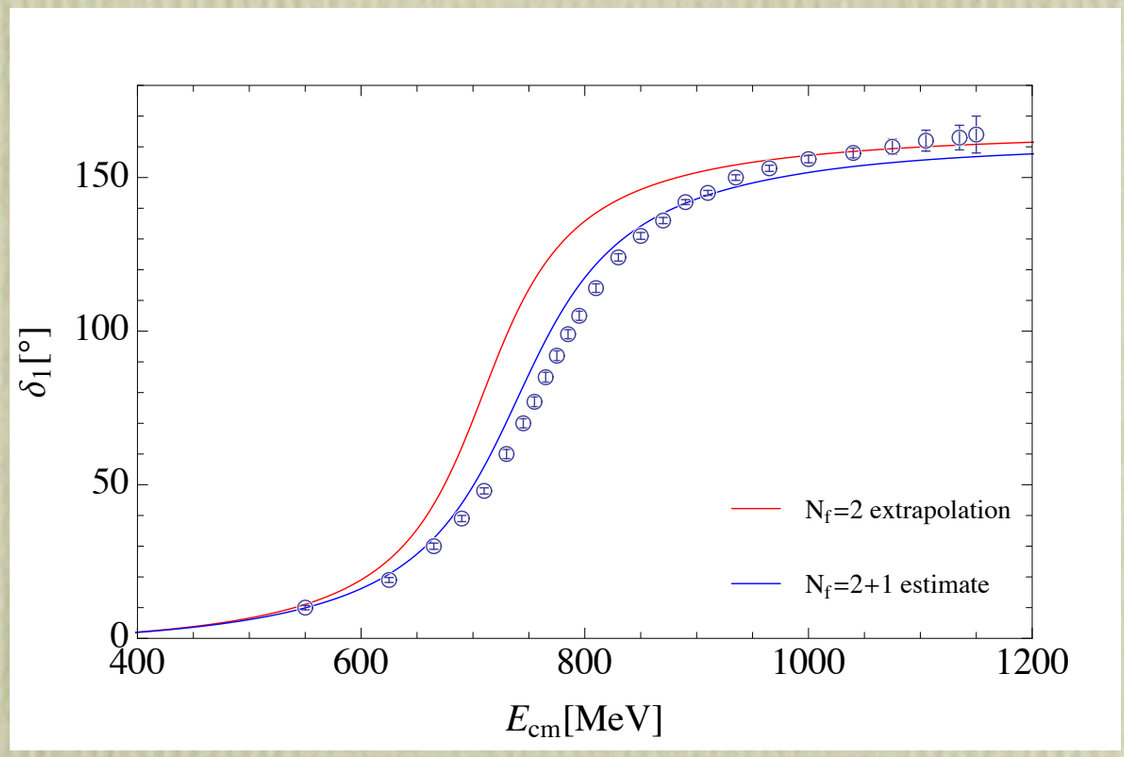

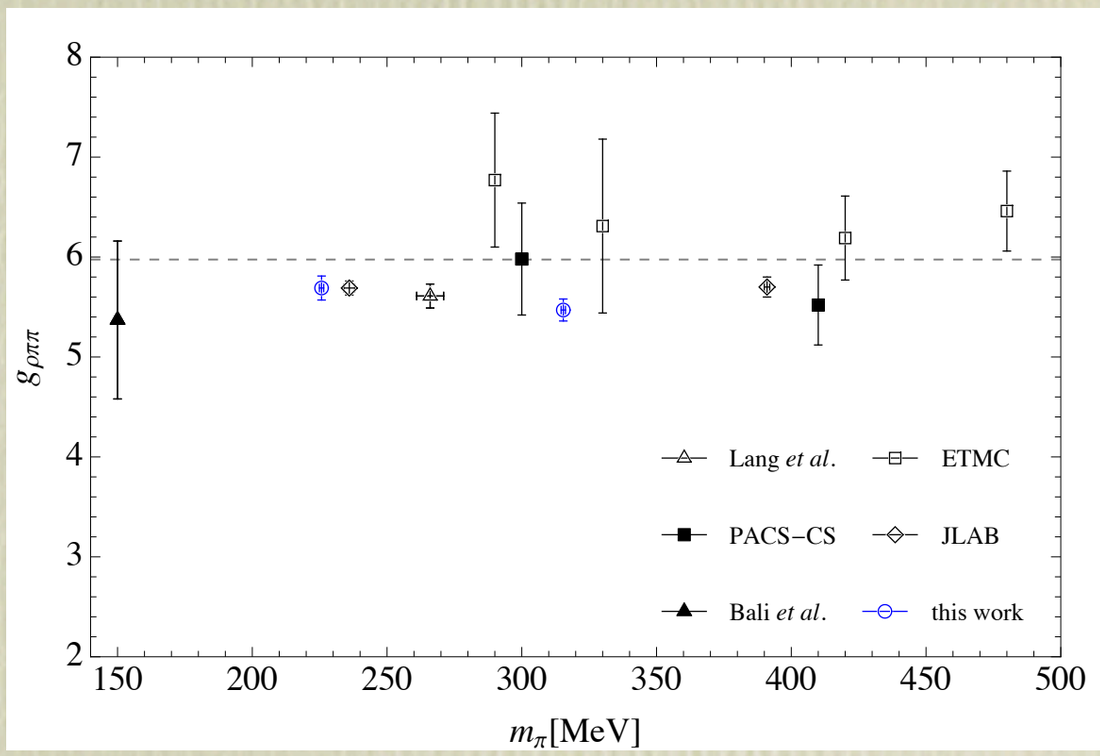

C. Pelissier and AA, Phys.Rev. D87 (2013) 014503, [arXiv:1211.0092].

D. Guo, AA, R. Molina, and M. Doering, Phys. Rev. D94 (2016), no. 3 034501, [arXiv:1605.03993].

ϱ-mass chiral extrapolation

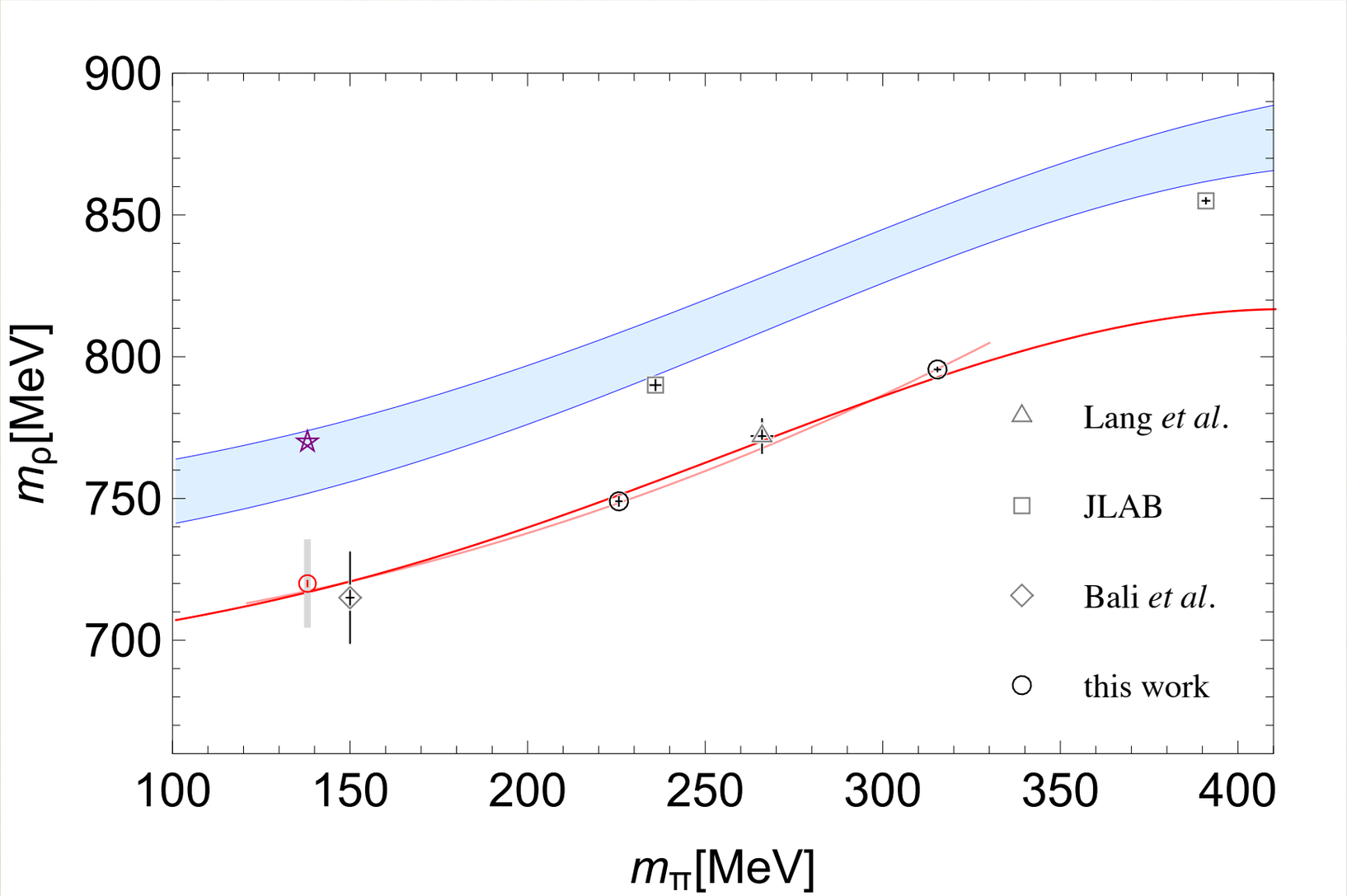

B. Hu, R. Molina, M. Doering, and AA, Phys. Rev. Lett. 117 (2016), no. 12 122001, [arXiv:1605.04823]

D. Guo, AA, R. Molina, and M. Doering, Phys. Rev. D94 (2016), no. 3 034501, [arXiv:1605.03993].

$$I=0$$

Operator basis - I=0

$$\sigma(\Gamma_i(\boldsymbol{p}),t) = \frac{1}{\sqrt{2}}[\bar{u}(t)\Gamma_i(\boldsymbol{p})u(t) + \bar{d}(t)\Gamma_i(\boldsymbol{p})d(t)]$$

i	$\Gamma_i(\boldsymbol{p})$	$\Gamma'_i(\boldsymbol{p})$
1	$\mathbf{1}e^{i\boldsymbol{p}}$	$\mathbf{1}e^{-i\boldsymbol{p}}$
2	$\nabla_i \mathbf{1} e^{i\boldsymbol{p}} \nabla_i$	$\nabla_i \mathbf{1} e^{-i\boldsymbol{p}} \nabla_i$
3	$\nabla_i^4 \mathbf{1} e^{i\boldsymbol{p}} \nabla_i^4$	$\nabla_i^4 \mathbf{1} e^{-i\boldsymbol{p}} \nabla_i^4$
4	$\gamma_i e^{i\boldsymbol{p}} \nabla_i$	$\gamma_i e^{-i\boldsymbol{p}} \nabla_i$

$$\pi\pi(\boldsymbol{p}_1,\boldsymbol{p}_2) = \frac{1}{\sqrt{3}}\{\pi^+(\boldsymbol{p}_1)\pi^-(\boldsymbol{p}_2) + \pi^-(\boldsymbol{p}_1)\pi^+(\boldsymbol{p}_2) + \pi^0(\boldsymbol{p}_1)\pi^0(\boldsymbol{p}_2)\}$$

- These are operators with I=0 and I_3=0.
- Linear combinations that change under $\mathbf{A_1}^+$ are used.

Spectrum

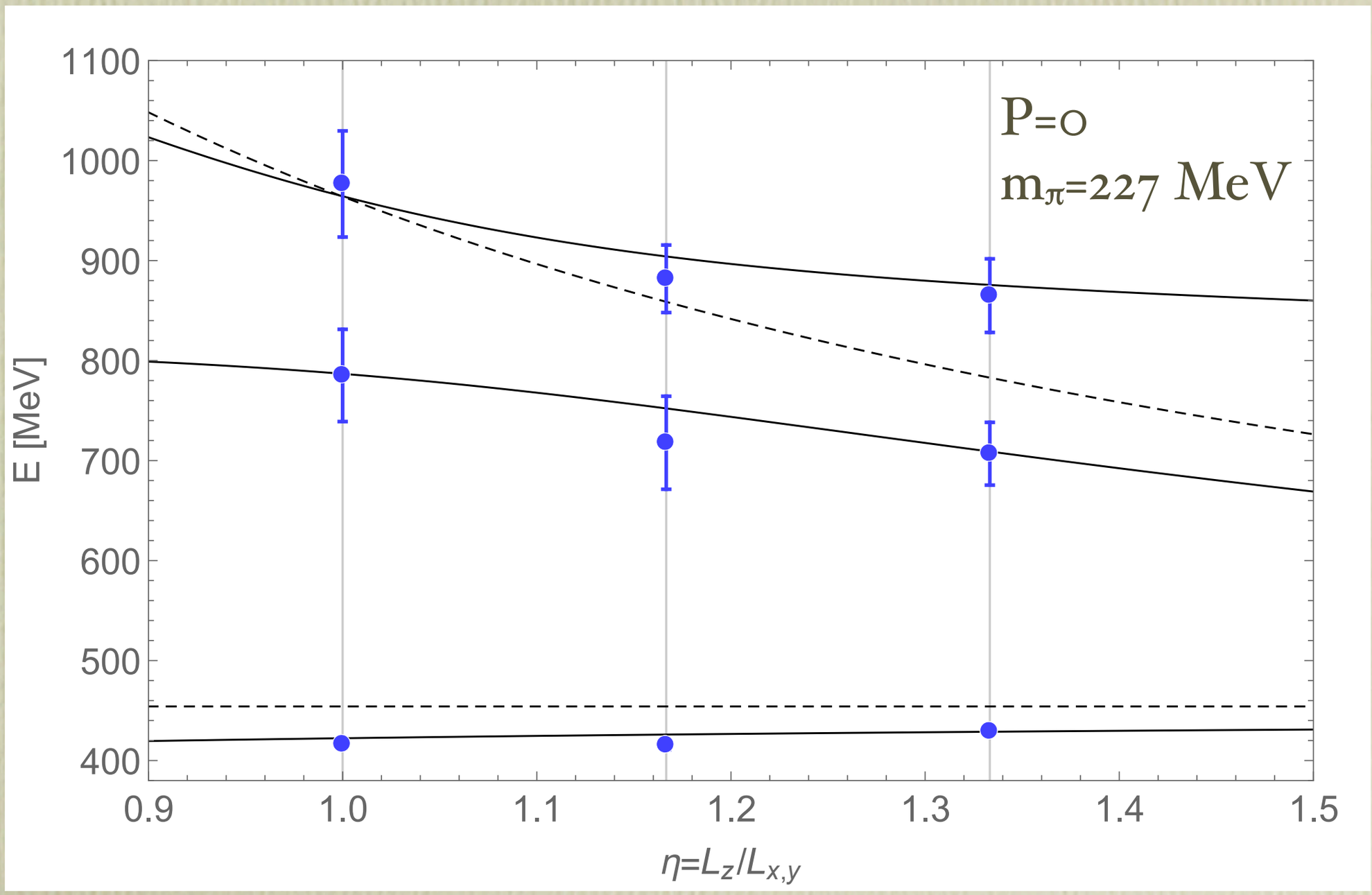

D. Guo, AA, R. Molina, M. Mai, and M. Döring, Phys. Rev. D98 (2018), no. 1 014507, [arXiv:1803.02897].

I=0 phase shifts—K-matrix fits

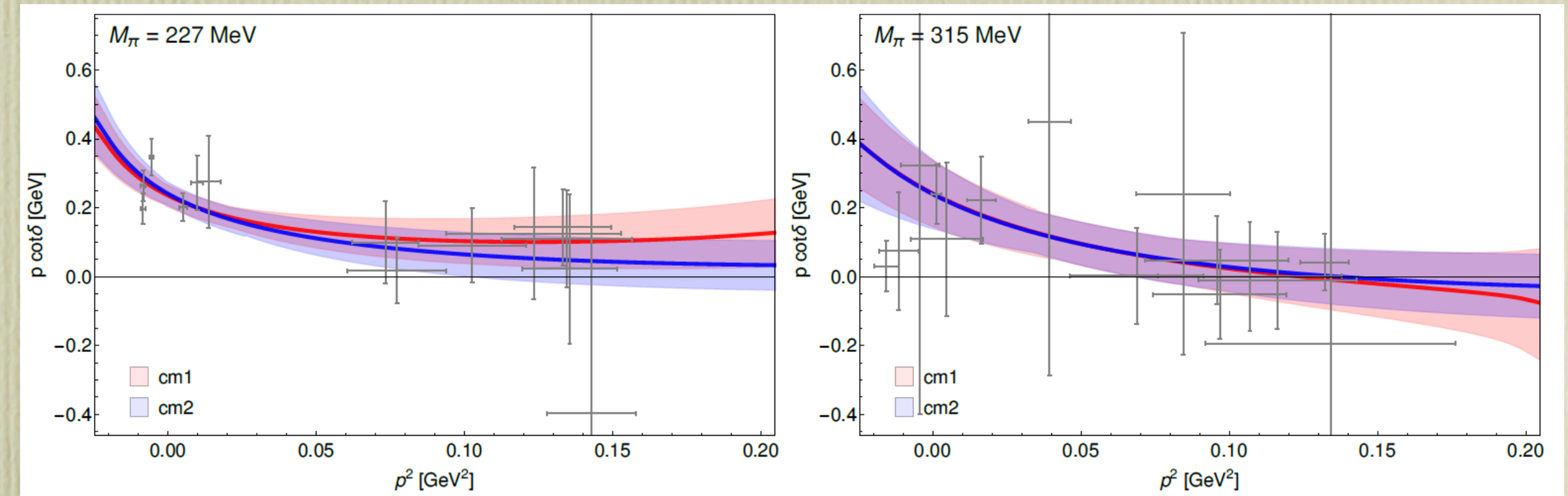

$$K_{00}^{-1}(s) = \frac{1}{16\pi}\frac{M_\pi^2}{s_A - s}\left(\frac{2s_A}{M_\pi\sqrt{s}} + B_0 + B_1\omega(s)\right)$$

$$\omega^{[\mathrm{cm1}]}(s) = \frac{\sqrt{s} - \alpha\sqrt{s_{\mathrm{thres}} - s}}{\sqrt{s} + \alpha\sqrt{s_{\mathrm{thres}} - s}}$$

$$\omega^{[\mathrm{cm2}]}(s) = \frac{\sqrt{s} - \sqrt{c}}{\sqrt{s} + \sqrt{c}}$$

I. Caprini, Phys. Rev. D77, 114019 (2008)

F. J. Yndurain, R. Garcia-Martin, and J. R. Pelaez, Phys. Rev. D76, 074034 (2007).

I=0 phase shifts—UχPT fits

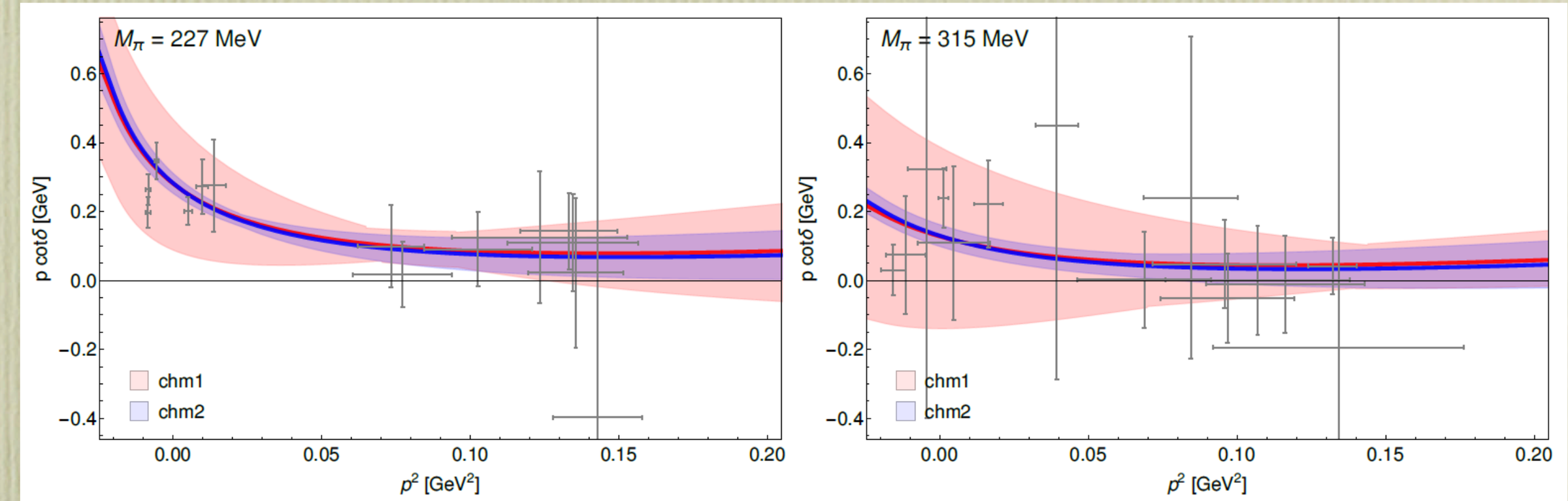

$$K_{00}(s) = \frac{3(M_\pi^2 - 2s)^2}{6f_\pi^2(M_\pi^2 - 2s) + 8(L_a M_\pi^4 + s(L_b M_\pi^2 + L_c s))}\,, \qquad K_{11}(s) = \frac{4M_\pi^2 - s}{3(f_\pi^2 - 8\,\hat{l}_1 M_\pi^2 + 4\,\hat{l}_2 s)}\,,$$

J. A. Oller, E. Oset, and J. R. Pelaez, Phys. Rev. D59, 074001 (1999)

Extrapolated phase-shifts

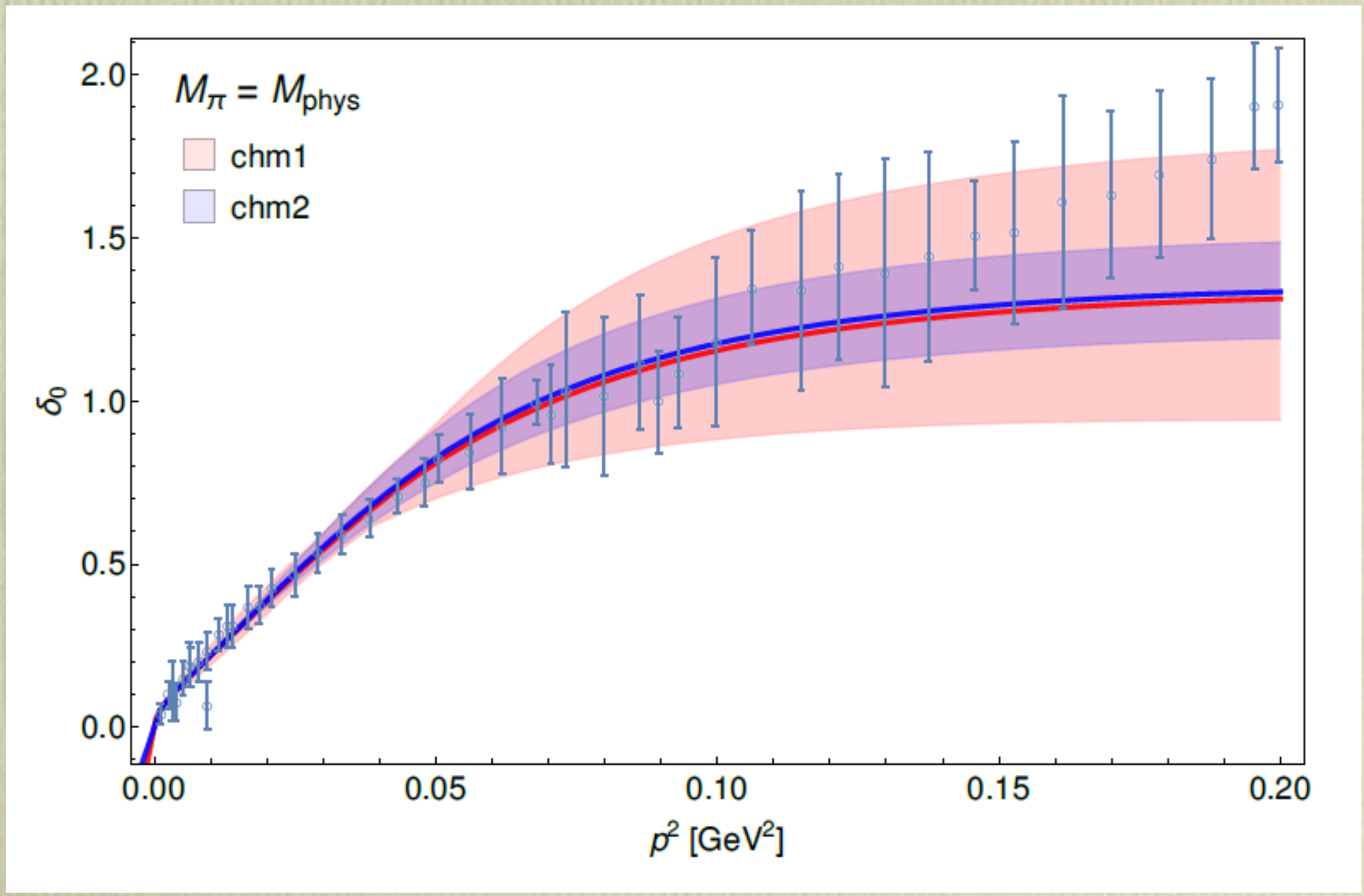

D. Guo, AA, R. Molina, M. Mai, and M. Döring, Phys. Rev. D98 (2018), no. 1 014507, [arXiv:1803.02897].

σ pole position and residue

		$M_\pi = 138$ MeV			$M_\pi = 227$ MeV			$M_\pi = 315$ MeV		
Parametrization	Fitted data	$\mathrm{Re}\, z^*$	$-\mathrm{Im}\, z^*$	g	$\mathrm{Re}\, z^*$	$-\mathrm{Im}\, z^*$	g	$\mathrm{Re}\, z^*$	$-\mathrm{Im}\, z^*$	g
cm1	σ_{227}	–	–	–	460^{+30}_{-60}	180^{+30}_{-30}	$3.2^{+0.1}_{-0.1}$	–	–	–
cm1	σ_{315}	–	–	–	–	–	–	660^{+50}_{-70}	150^{+40}_{-50}	$4.0^{+0.2}_{-0.2}$
cm2	σ_{227}	–	–	–	475^{+30}_{-60}	176^{+50}_{-40}	$3.3^{+0.3}_{-0.2}$	–	–	–
cm2	σ_{315}	–	–	–	–	–	–	660^{+50}_{-90}	140^{+40}_{-50}	$3.9^{+0.2}_{-0.2}$
chm1	$\sigma_{227,315}$	440^{+60}_{-90}	240^{+20}_{-50}	$3.0^{+0.2}_{-0.6}$	490^{+100}_{-70}	170^{+40}_{-110}	$3.0^{+0.7}_{-0.5}$	590^{+130}_{-120}	80^{+150}_{-80}	$4.0^{+4.0}_{-2.0}$
chm2	σ_{227} ρ_{227}	430^{+20}_{-30}	250^{+30}_{-30}	$3.0^{+0.1}_{-0.1}$	460^{+30}_{-40}	160^{+30}_{-30}	$3.0^{+0.1}_{-0.1}$	620^{+10}_{-80}	0^{+60}_{-0}	$3.1^{+6.0}_{-3.0}$
chm2	σ_{315} ρ_{315}	460^{+10}_{-15}	210^{+40}_{-30}	$3.0^{+0.1}_{-0.1}$	540^{+30}_{-40}	150^{+30}_{-30}	$3.1^{+0.1}_{-0.1}$	660^{+40}_{-60}	120^{+40}_{-40}	$3.6^{+0.1}_{-0.1}$
chm2	$\sigma_{227,315}$ $\rho_{227,315}$	440^{+10}_{-16}	240^{+20}_{-20}	$3.0^{+0.0}_{-0.0}$	500^{+20}_{-20}	160^{+15}_{-15}	$3.0^{+0.0}_{-0.1}$	600^{+30}_{-40}	80^{+20}_{-80}	$3.9^{+5.0}_{-0.2}$
Ref. [1]	experimental	449^{+22}_{-16}	275^{+12}_{-12}	$3.5^{+0.3}_{-0.2}$	–	–	–	–	–	–

D. Guo, AA, R. Molina, M. Mai, and M. Döring, Phys. Rev. D98 (2018), no. 1 014507, [arXiv:1803.02897].

σ pole position and residue

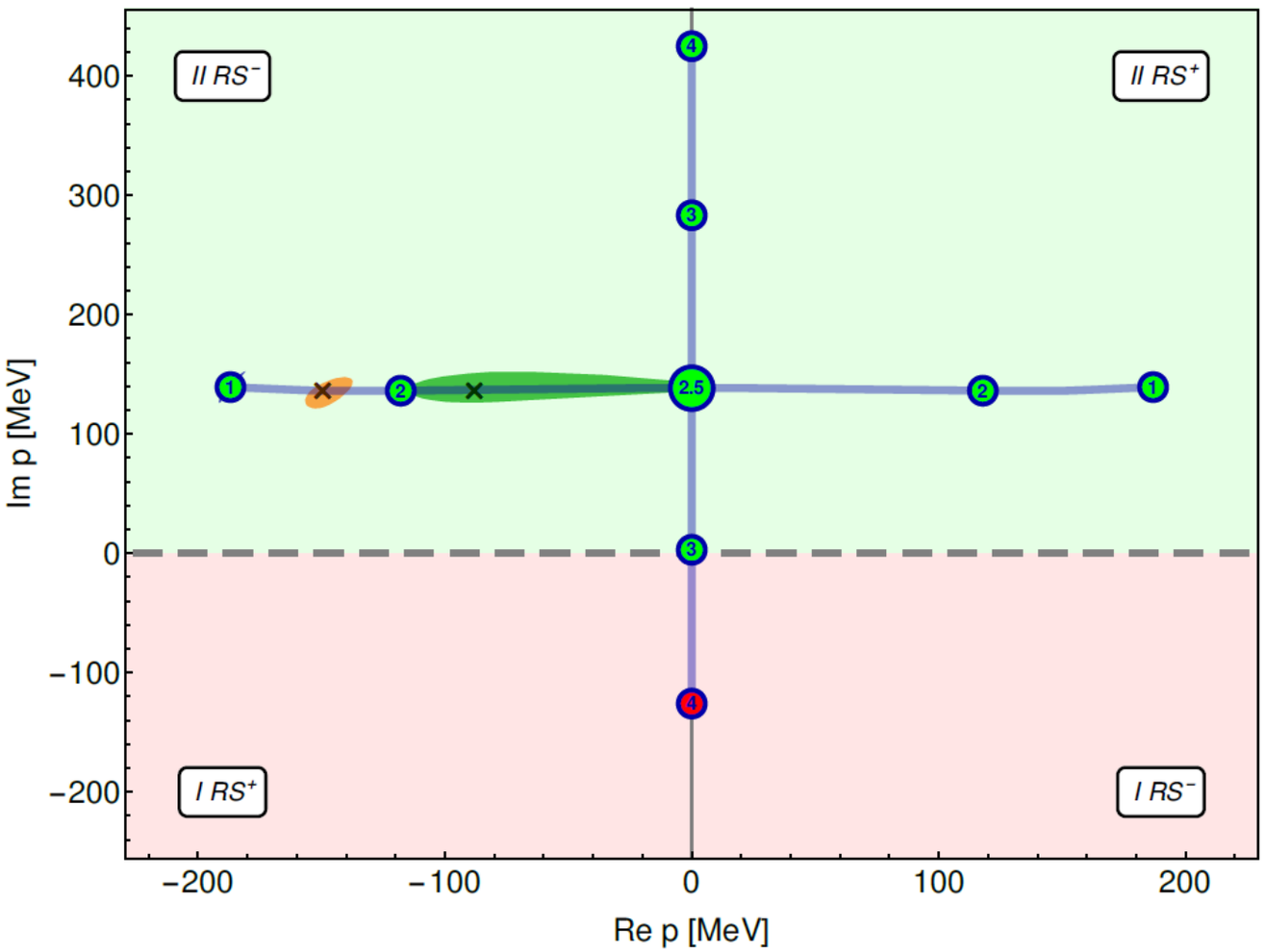

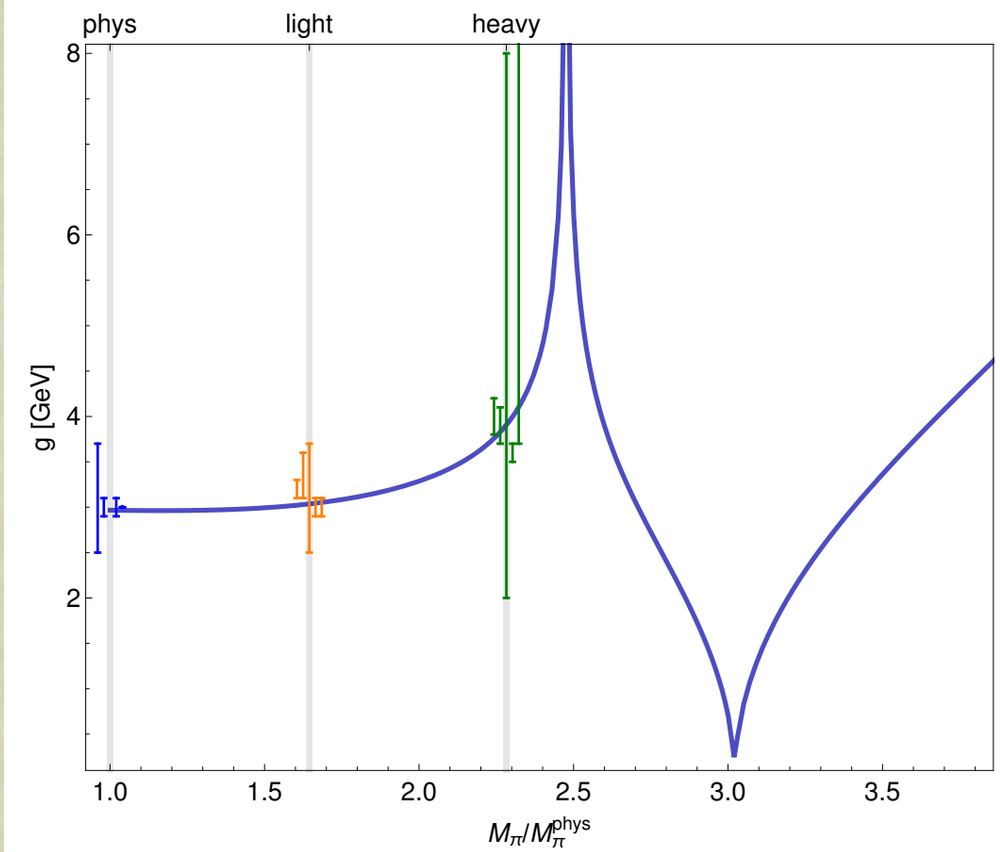

D. Guo, AA, R. Molina, M. Mai, and M. Döring, Phys. Rev. D98 (2018), no. 1 014507, [arXiv:1803.02897].

$$I=2$$

Energy levels

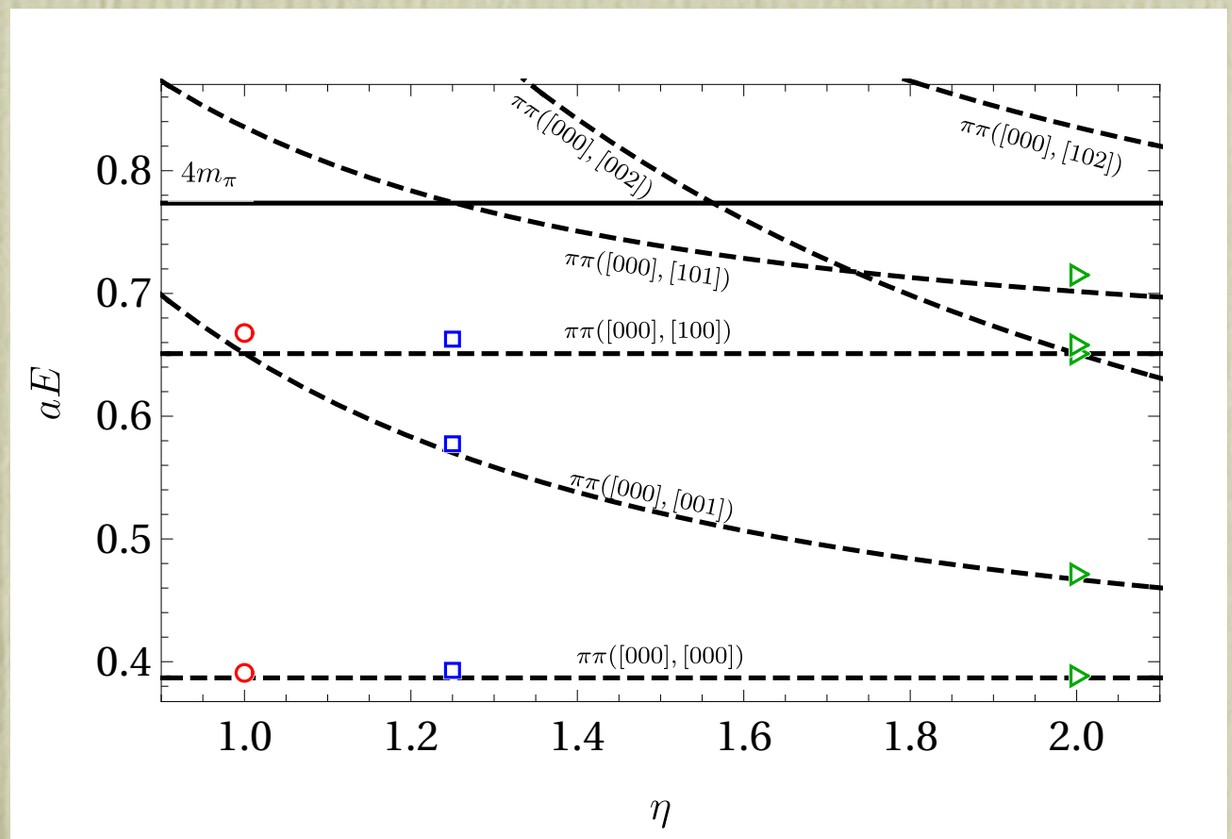

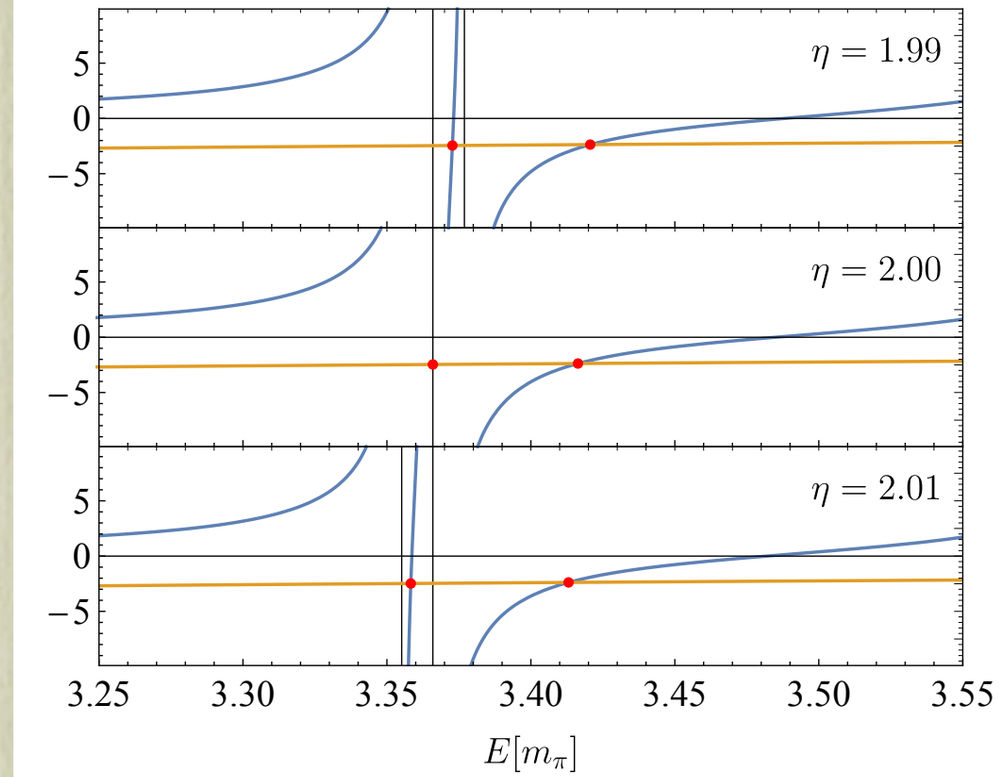

C. Culver, M. Mai, AA, M. Dring, and F. X. Lee, Phys. Rev. D100 (2019), no. 3 034509, [arXiv:1905.10202].

Phase shifts

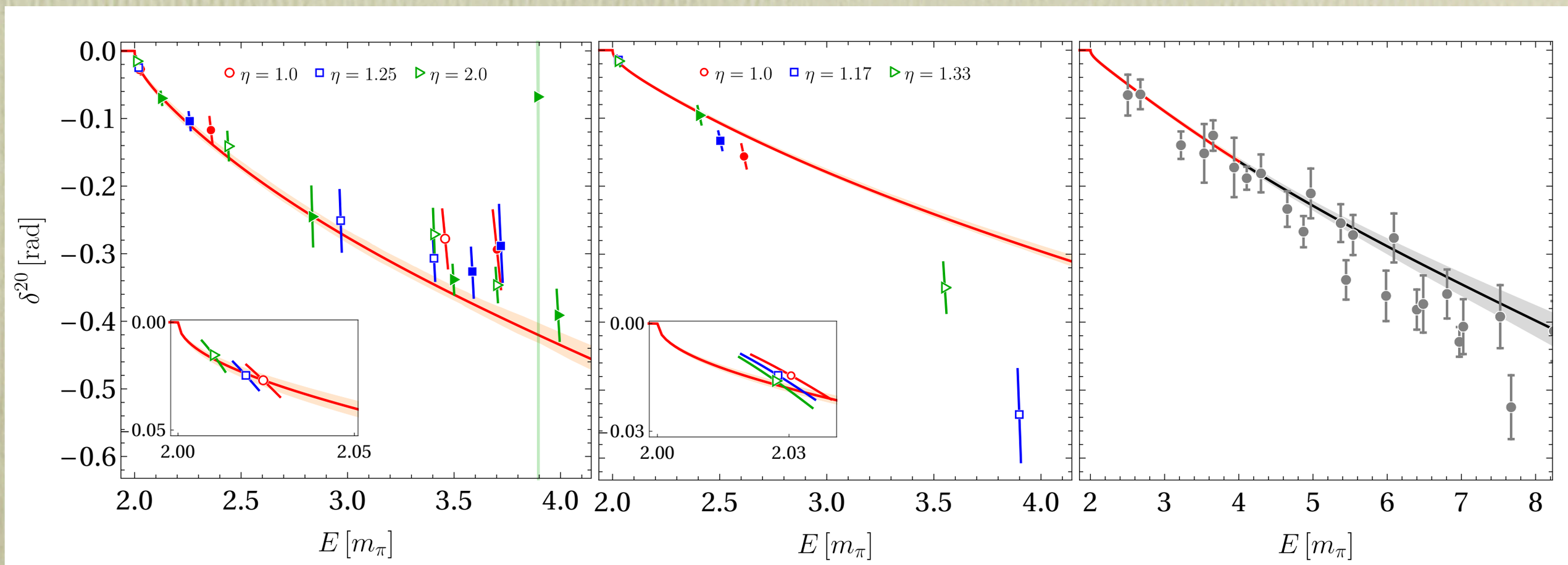

C. Culver, M. Mai, AA, M. Dring, and F. X. Lee, Phys. Rev. D100 (2019), no. 3 034509, [arXiv:1905.10202].

Global fit

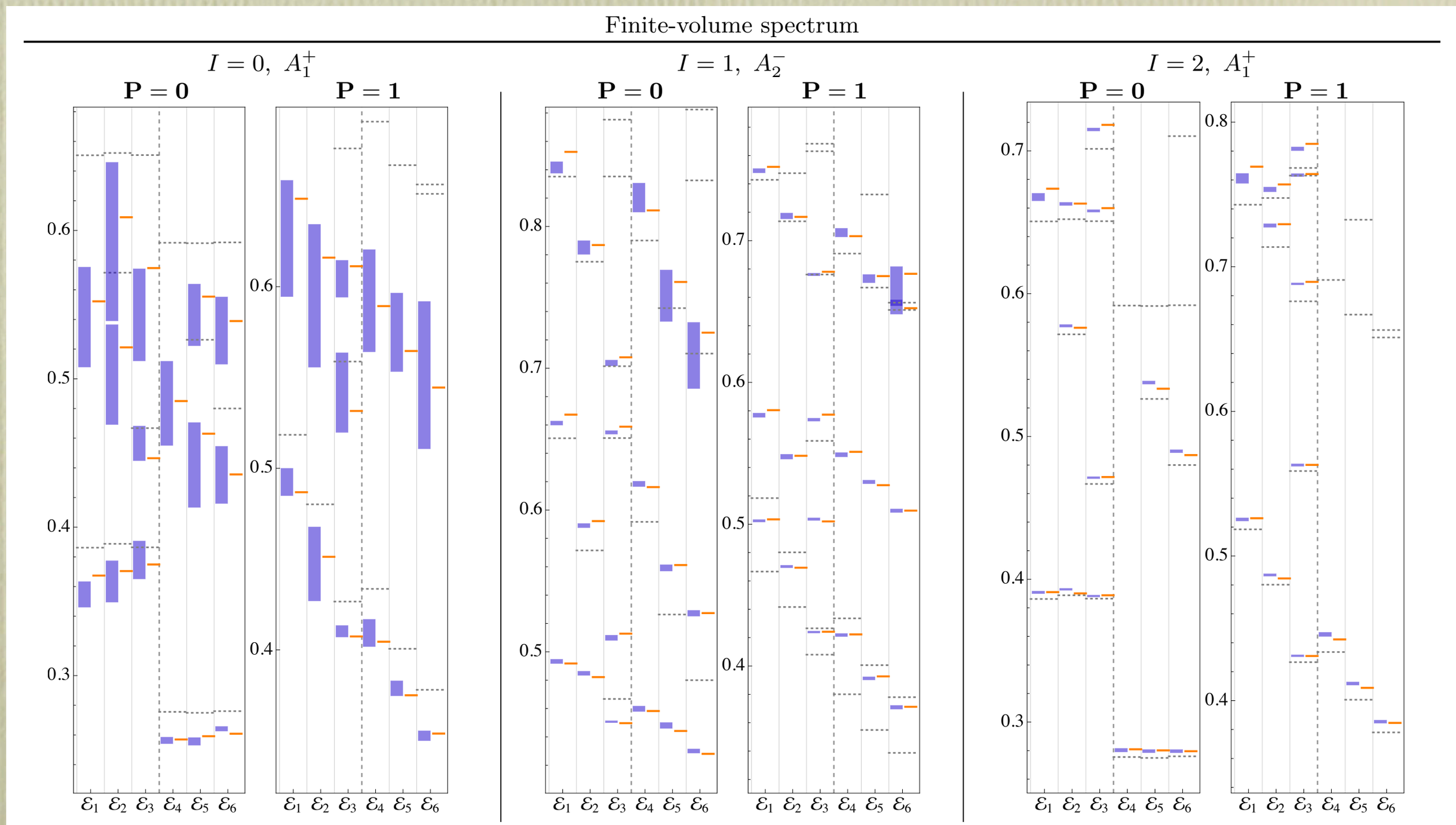

M. Mai, C. Culver, AA, M. Dring, and F. X. Lee, A cross-channel study of pion scattering from lattice QCD, arXiv:1908.01847.

Global fit

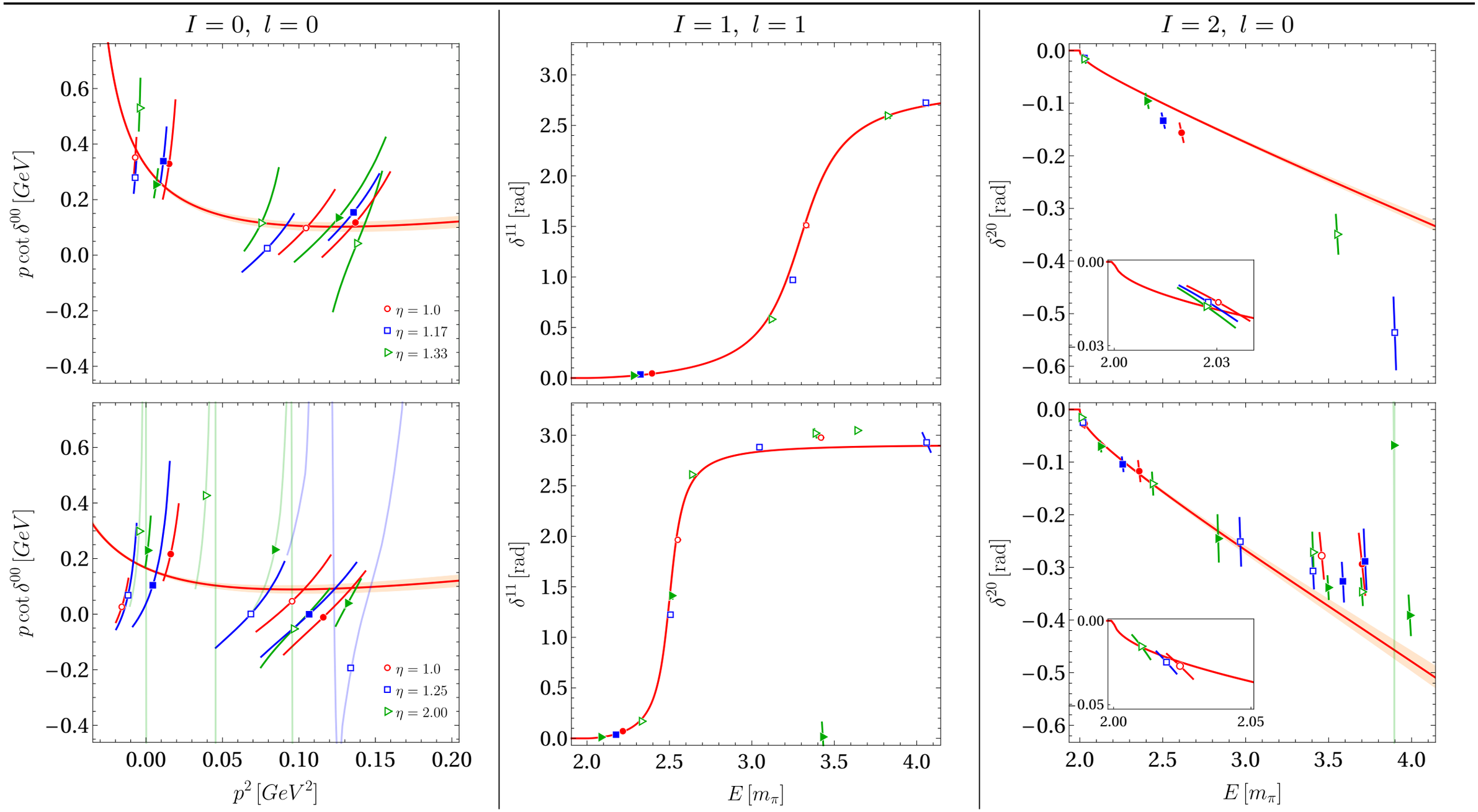

M. Mai, C. Culver, AA, M. Dring, and F. X. Lee, A cross-channel study of pion scattering from lattice QCD, arXiv:1908.01847.

Global fit

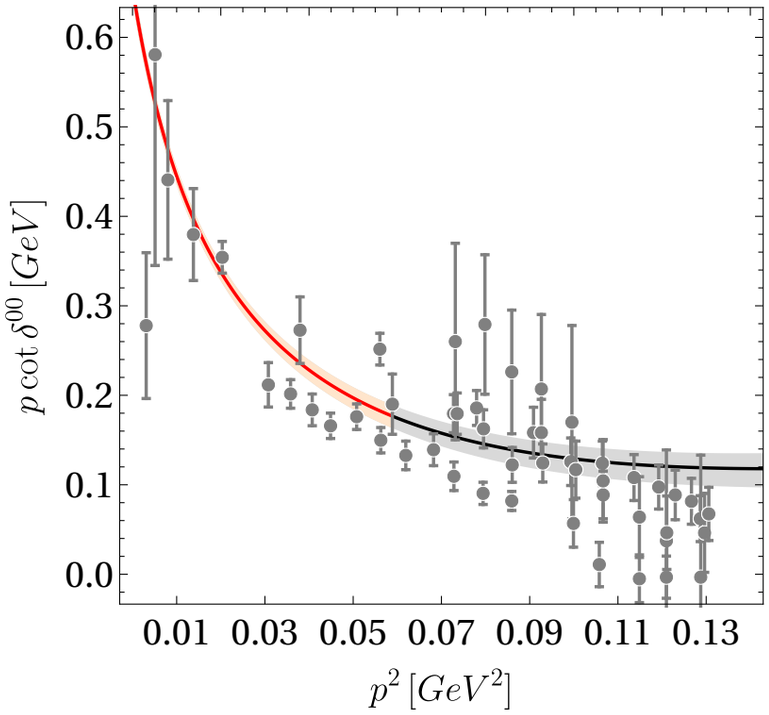

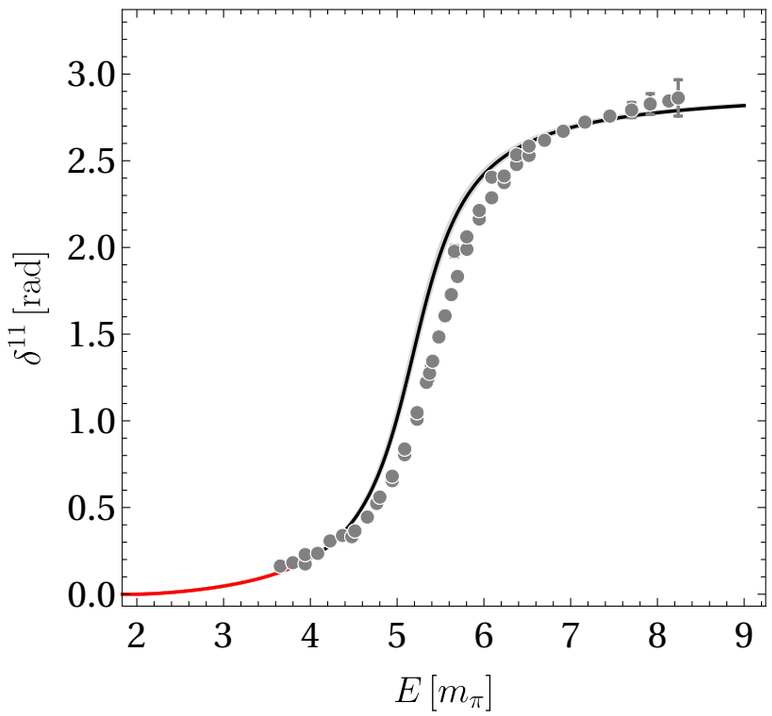

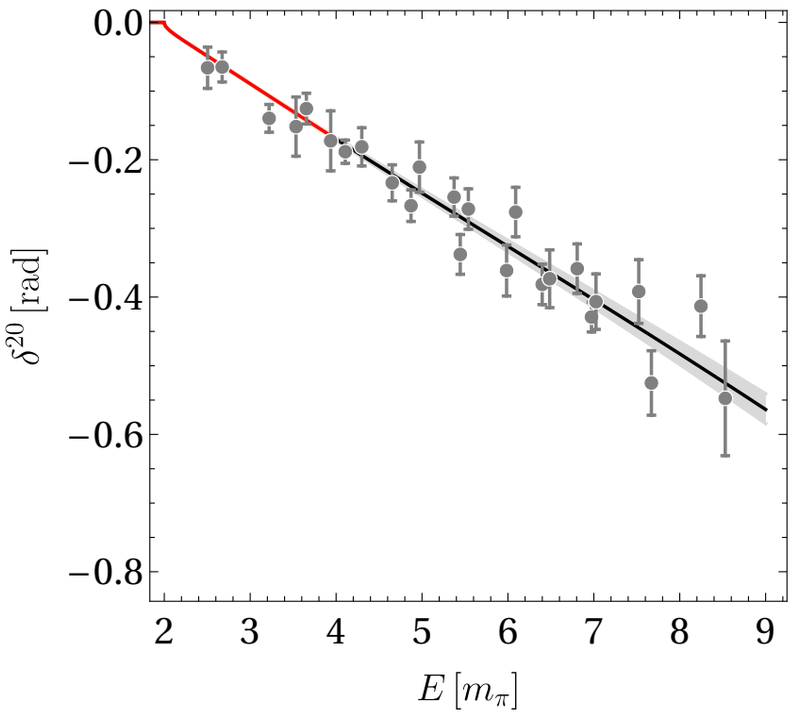

M. Mai, C. Culver, AA, M. Dring, and F. X. Lee, A cross-channel study of pion scattering from lattice QCD, arXiv:1908.01847.

Conclusions and outlook

- We performed a lattice Nf=2 QCD calculation for the phase shifts in the I=0,1,2 channel in the elastic region. We use zero-momentum and boosted states at m_π=227 and m_π=315 MeV. We use elongated boxes as an efficient way to access a larger kinematic range.

- We fitted a number of models to the phase-shifts and identified the position of the ϱ and σ resonances.

- We used Unitarized χPT model to extrapolate to physical pion mass and we for find for σ a value consistent with experimental analysis and for ϱ a value significantly smaller than the experimental one. We argued that the ϱ mass discrepancy is due to the absence of the strange quarks.

- In general we find that Unitarized χPT describes the data qualitatively very well but there is some tension between the lattice data and the model. Further studies are required to determine whether the tension is due to lattice systematics or model deficiencies.

- **Outlook**: refine our methods to increase both the precision and the range of our phase shift calculation (with an eye on $f_0(980)$), compute three body energies, move towards lower quark masses, investigate the continuum limit.